



January 16, 2019

Dear Senate and House Transportation Committee Leadership and Members:

Please find attached the University of Washington's research and development study regarding expansion joint noise on WSDOT bridges. The Legislature provided funding to WSDOT in the 2018 supplemental transportation budget to contract with the UW to study expansion joint noise. The text, included in ESSB 6106, is as follows:

*Section 218 (3): \$181,000 of the motor vehicle account state appropriation is provided solely for the department, in coordination with the University of Washington department of mechanical engineering, to study measures to reduce noise impacts from bridge expansion joints. The study must examine testing methodologies and project timelines and costs. A final report must be submitted to the transportation committees of the legislature by October 15, 2018.*

The impetus for this funding was to help address community concerns raised regarding noise generated by bridge joints. In 2016, this concern was highlighted by the opening of the new SR 520 floating bridge. At that time, WSDOT began investigations into the noise levels coming from the new bridge. In May 2017, WSDOT published a [white paper](#) including noise measurements, existing noise reduction measures built into the new bridge, potential pilot project study options, and estimated costs to conduct a pilot project. The white paper also noted that the SR 520 floating bridge meets all current state and FHWA criteria for noise abatement.

WSDOT has over 50 bridges with modular expansion joints which allow bridge movements from the low end of six inches to over four feet for the large SR 520 modular expansion joints. While the large modular expansion joints on SR 520 are quieter than similar expansion joints on the I-90 Floating Bridge, the intent of this research was to examine options to reduce noise on modular expansion joints including those found on the SR 520 bridge. Please let me know if you have any questions.

Sincerely,

A handwritten signature in black ink, appearing to read 'R. Millar'.

Roger Millar, PE, FASCE, FAICP  
Secretary of Transportation

CC: Mark Gaines, WSDOT Bridge and Structures Engineer  
Cody Elwell, University of Washington

**Research Report**  
Expansion Joint Noise

# Modular Expansion Joint Noise Mitigation Study

By

Per G. Reinhall and Alexander G. Soloway

Department of Mechanical Engineering  
University of Washington  
Seattle, Washington 98105-6698

**Prepared for**  
The State of Washington  
Department of Transportation

January 14, 2019

## Table of Contents

<b>1</b>	<b><i>Introduction</i></b> .....	<b>1</b>
<b>2</b>	<b><i>Background</i></b> .....	<b>2</b>
2.1	<b>Noise Generating Mechanisms</b> .....	<b>2</b>
2.2	<b>Noise Abatement Options</b> .....	<b>3</b>
<b>3</b>	<b><i>Experiment Description</i></b> .....	<b>5</b>
3.1	<b>Site Description</b> .....	<b>5</b>
3.2	<b>Existing Noise Abatement Measures</b> .....	<b>7</b>
3.3	<b>Residential Measurements October 18, 2018</b> .....	<b>7</b>
3.4	<b>Bridge Measurements</b> .....	<b>8</b>
3.4.1	<b>East Side Joint Measurements October 23, 2018</b> .....	<b>8</b>
3.4.2	<b>West Side Joint Measurements November 1, 2018</b> .....	<b>8</b>
3.4.3	<b>East Side Joint Measurements November 7, 2018</b> .....	<b>8</b>
3.4.4	<b>West Side Joint Measurements November 8, 2018</b> .....	<b>9</b>
<b>4</b>	<b><i>Methodology</i></b> .....	<b>10</b>
4.1	<b>Equipment Description</b> .....	<b>10</b>
4.2	<b>Data Processing</b> .....	<b>11</b>
<b>5</b>	<b><i>Results and Discussion</i></b> .....	<b>12</b>
5.1	<b>Residential Locations</b> .....	<b>13</b>
5.2	<b>Joint Measurements</b> .....	<b>15</b>
5.3	<b>Measurements Above and Below Expansion Joint</b> .....	<b>18</b>
5.4	<b>Directionality of Noise Above Joint</b> .....	<b>20</b>
5.5	<b>Tire Size Comparison</b> .....	<b>22</b>
5.6	<b>Sinus Plates</b> .....	<b>24</b>
5.7	<b>High-Speed Camera Measurements</b> .....	<b>25</b>
5.8	<b>Noise Abatement Options</b> .....	<b>29</b>
<b>6</b>	<b><i>Summary and Recommendations</i></b> .....	<b>31</b>
6.1	<b>Summary and Recommendations for SR520 Bridge</b> .....	<b>31</b>
6.2	<b>General Conclusions for All Modular Expansion Joint</b> .....	<b>31</b>
6.3	<b>General Recommendations</b> .....	<b>32</b>
	<b><i>References</i></b> .....	<b>33</b>
	<b><i>Appendix A. Tire Width Study</i></b> .....	<b>34</b>
	<b><i>Appendix B. Golden Ears Bridge Maintenance Report</i></b> .....	<b>45</b>

## Table of Figures

Figure 3-1: West-side measurement site (map from Google Earth) .....	6
Figure 3-2: East-side measurement site (map from Google Earth).....	6
Figure 5-1: Overview of car-pass events using simultaneous noise and video recordings. Screen-shots from the video are attributed to specific parts of the noise recording using letters (A)-(I).....	13
Figure 5-2: Equipment setup at (a) 2839 Evergreen Point Road, (B) 3221 Evergreen Point Road, and (C) view of expansion joint and sentinel on east side of bridge from 3221 Evergreen Point Road.....	14
Figure 5-3: Average ESD of measurements collected at (a) 2839 Evergreen Point Road and (b) 3221 Evergreen Point Road .....	14
Figure 5-4: (A) Schematic of equipment setup for the single receiver measurements at the large expansion joints on the east and west sides of the bridge, and (B) Equipment setup at the large expansion joint on the east side of the floating bridge from the pedestrian walkway.....	16
Figure 5-5: Spectral average of car pass events on October 23, 2018 and November 7, 2018 at the east side expansion joint (thick orange) and car pass events on November 1, 2018 and November 8, 2018 on the west-side expansion joint (thin blue line). The background levels are also shown for both expansion joints. ....	16
Figure 5-6: Time series (blue) of a single car-pass event centered at 0.0 s and the time samples used for calculating the ESD of the background noise (red) .....	17
Figure 5-7: Equipment setup for simultaneous measurements collected above the expansion joint and in the joint cavity. ....	18
Figure 5-8: Equipment setup below the west-side large expansion joint with receivers east and west of the joint cavity. ....	18
Figure 5-9: Comparison of ESD for noise measured above the joint and below in the joint cavity for the (a) east-side joint and (b) the west side joint. ....	19
Figure 5-10: ESD of car-pass events measured below the west-side joint on the east and west side of the joint cavity. The west side of the joint cavity faces the transition span and has openings whereas the east side of the joint cavity is fully enclosed. These data are compared to the average ESD measured above the road and in the joint cavity. ....	20
Figure 5-11: Equipment setup for measurements on the east and west side of the large modular expansion joints. ....	21
Figure 5-12: Measurements collected east and west of (a) the west-side large expansion joint with a receiver offset of 10 m, (b) the west-side large expansion joint with a receiver offset of 20 m, and (c) the east-side large expansion joint with a receiver offset of 24 m. ....	22
Figure 5-13: ESD of individual car-pass events (blue) compared to the resonance frequency associated with the car tire width. The resonance frequencies determined by Eq.(2) that are associated range of tire widths (highlighted in magenta) were identified using the minimum and maximum tire widths from manufacturer specifications of various body style and trim level. To provide a clearer relationship between the tire width and peak ESD, the broadband spectra have also been smoothed using a Savitzky-Golay filter (orange) to highlight the overall trend of the ESD.....	23
Figure 5-14: Volume formed by car tires rolling over gap between center beam. Resonance frequency determined by selecting L in Eq. (2) to be the width of the tire, $W_t$ . ....	24
Figure 5-15: Average ESD of car pass events measured at the small expansion joint with sinus plates on the west approach bridge compared to large expansion joints on east and west sides of the floating bridge.....	25
Figure 5-16 Frame from high-speed video recording of Toyota Prius front tire passing over east-side large expansion joint center beams. ....	26
Figure 5-17 Frame from high-speed video recording of a Scion sports car front tire passing over east-side large expansion joint center beams. ....	26
Figure 5-18 Frame from high-speed video recording of an SUV tire passing over east-side large expansion joint center beams. ....	27

Figure 5-19 Frame from high-speed video recording of a Toyota Tundra front tire passing over east-side large expansion joint center beams. ....	27
Figure 5-20 Frame from high-speed video recording of a car-carrier truck front tire passing over east-side large expansion joint center beams. ....	28
Figure 5-21 Frame from high-speed video recording of a bus front tire passing over east-side large expansion joint center beams. ....	28
Figure 5-22: Average ESD for varying vehicle types (sedan, SUV, truck and bus) using data collected at the east-side large expansion joint on October 23, 2018 and November 7, 2018 and at the west-side large expansion joint on November 1, 2018 and November 8, 2018.....	29
Figure A-1: ESD of car pass events (blue) and ESD with Savitsky-Golay smoothing filter (orange) compared to resonance frequency calculated using Eq. (2). ....	34
Figure A-2: ESD of car pass events (blue) and ESD with Savitsky-Golay smoothing filter (orange) compared to resonance frequency calculated using Eq. (2) .....	35
Figure A-3: ESD of car pass events (blue) and ESD with Savitsky-Golay smoothing filter (orange) compared to resonance frequency calculated using Eq. (2) .....	36
Figure A-4: ESD of car pass events (blue) and ESD with Savitsky-Golay smoothing filter (orange) compared to resonance frequency calculated using Eq. (2) .....	37
Figure A-5: ESD of car pass events (blue) and ESD with Savitsky-Golay smoothing filter (orange) compared to resonance frequency calculated using Eq. (2) .....	38
Figure A-6: ESD of car pass events (blue) and ESD with Savitsky-Golay smoothing filter (orange) compared to resonance frequency calculated using Eq. (2) .....	39
Figure A-7: ESD of car pass events (blue) and ESD with Savitsky-Golay smoothing filter (orange) compared to resonance frequency calculated using Eq. (2) .....	40
Figure A-8: ESD of car pass events (blue) and ESD with Savitsky-Golay smoothing filter (orange) compared to resonance frequency calculated using Eq. (2) .....	41
Figure A-9: ESD of car pass events (blue) and ESD with Savitsky-Golay smoothing filter (orange) compared to resonance frequency calculated using Eq. (2) .....	42
Figure A-10: ESD of car pass events (blue) and ESD with Savitsky-Golay smoothing filter (orange) compared to resonance frequency calculated using Eq. (2) .....	43
Figure A-11: ESD of car pass events (blue) and ESD with Savitsky-Golay smoothing filter (orange) compared to resonance frequency calculated using Eq. (2) .....	44

# 1 Introduction

The noise created by vehicles driving over modular expansion joints is a nuisance to residents in several parts of the State of Washington, with the Washington State Department of Transportation (WSDOT) receiving noise complaints from bridges throughout the state. Large expansion joints in particular have been problematic, such as those installed on the Evergreen Point Floating Bridge (SR520 bridge). Shortly after opening in 2016, WSDOT started receiving noise complaints relating to the large, 16 center beam, expansion joints on the east and west ends.

While several studies have investigated the noise from modular expansion joints, most have focused on low frequency noise (below 200 Hz) radiated from the underside of the bridge [1]–[5]. Several technologies to reduce expansion joint noise are currently available, however the available literature on the subject does not discuss what noise mechanism(s) the mitigation options address nor their effectiveness. In this report the existing noise nuisance from the SR520 bridge expansion joints is used as a case study to collect information on the noise from modular expansion joints to better understand the noise generating mechanisms. Funding for this project was provided by the Washington State Legislature with \$181,000 of the motor vehicle account-state appropriation provided solely for WSDOT, in coordination with the University of Washington department of mechanical engineering, to study measures to reduce noise impacts from bridge expansion joints. The primary goals of this report are

- Investigate the mechanism(s) responsible for the expansion joint noise including their spectral characteristics and their point of origin.
- Summarize existing mitigation options for controlling noise from modular expansion joints and consider each option within the context of the noise generating mechanisms they address.
- Guide an investigation of the durability, cost, and effectiveness of a practical mitigation solution with high potential to be implemented by WSDOT for existing or future bridges.

In addition to these primary goals, specific recommendations on the SR520 bridge will be presented including the origin of the noise that is the source of the noise complaints as well as potential noise mitigation options. The process developed during this project and recommendations in this report could be applied to other bridges that use modular expansion joints.

In the following report, background information will first be presented in Section 2 including a summary of noise abatement options and previous studies of expansion joint noise. The experimental description will then be provided in Section 3 followed by the methodology used to analyze these data in Section 4. The Results from the experiments will be presented in Chapter 5 along with a discussion on the results. Finally, a summary of the report with recommendations will be presented in Chapter 6.

## 2 Background

### 2.1 Noise Generating Mechanisms

The mechanisms responsible for the noise generated by cars passing over modular expansion joints fall into two categories; noise emanating from the cavity below a modular expansion joints and noise from the top of the joint [1]. The noise below the expansion joint will be presented first as it is the focus of all but one of the previous expansion joint noise studies. These studies [1]–[5], have used numerical modelling, full scale models and existing modular expansion joints to show that the impact of car tires on modular expansion joints cause the joint beams (both center beams and support beams) to vibrate. These vibrations then couple to acoustic modes of the joint cavity with resonant frequencies below 200 Hz. One of the mechanisms responsible for exciting the center beams is referred to as the bar-pass frequency,  $f_{bar}$ , which describes the frequency at which the car tires strike the center beams. It is given by

$$f_{bar} = \frac{V}{W_g + W_b} \quad (1)$$

Where  $V$  is the velocity of the car (m/s),  $W_g$  is the width of the gap between the center beams (m), and  $W_b$  is the width of the center beam (m). A resonance is excited when this frequency is equal to the vibration response of a center beam.

Compared to noise originating below the joint, comparatively little work has been devoted to investigating the noise from the top of the joint. One of the only studies addressing this topic is by Ravshanovich et. al [1] where noise up to 1000 from above and below the joint are compared. They also show that above 500 Hz sound levels from the top of the joint are significantly higher than those measured below the joint. These data show that the noise above the joint has a center frequency (maximum value) of 700 Hz. The authors explain that this is caused by resonances being excited in the gap formed by the rubber sealing and two adjacent center beams is covered by the car tire. The authors present data from a “car” and “sedan” that show differences in the center (or maximum) frequency which they attribute to differences in the tire widths. The authors, unfortunately, do not discuss this relationship in detail nor do they provide detailed information on the study that led to this conclusion. The relation between tire width and resonance frequency can potentially be determined using an equation from Ver and Beranek for the approximate resonance frequency in an arbitrary volume [6]

$$f_o = \frac{c}{2W} \quad (2)$$

Where  $f_o$  is the resonance frequency (Hz),  $c$  is the speed of sound in air (typically 340 m/s) and  $W$  is the largest dimension in the arbitrary volume. For this scenario,  $W$  is the width of the tire

(typically in the range of 185 mm and 305 mm). The relation between the tire width and Eq. (2) will be discussed in Section 5.5.

## 2.2 Noise Abatement Options

Existing abatement options to reduce the expansion joint noise are summarized in Table 1. These technologies fall into one of two categories; low frequency mitigation options to reduce noise levels below 400 Hz or high frequency options to reduce noise above 400 Hz. Noise barriers, which can reduce noise across a wide range of frequencies, can reduce noise both above and below 400 Hz; however, they are not effective in all situations and must provide line-of-sight coverage to be effective [7]. As most of these existing solutions apply to specific frequency ranges, the selection of an appropriate noise mitigation method first requires the noise source and character of the noise (spectrum of noise) to be identified. It should also be note that while Helmholtz resonators can be tuned to any frequency of interest, the study by Ancich [2] only discusses frequencies below 200 Hz.



Table 1: Summary of Noise Control Options

Noise Control	Frequency Range	Strength	Weakness	Reference
Noise Barrier	Broadband	<ul style="list-style-type: none"> <li>-mitigates noise originating from top of joint</li> <li>- reduces broadband noise for receivers close to the barrier</li> </ul>	<ul style="list-style-type: none"> <li>- Must extend enough to cover noise source</li> <li>- Reduction less at long distances</li> <li>- Can increase noise from reflections</li> <li>- Cannot control refraction effects</li> </ul>	Crocker [7]
Helmholtz Resonator in Joint Cavity	<200 Hz (tuned to specific frequencies)	<ul style="list-style-type: none"> <li>- Can be tuned to resonance frequencies of joint vibration</li> <li>- attenuate noise at specific, problematic frequencies</li> </ul>	<ul style="list-style-type: none"> <li>- Only reduce noise at specific frequencies its tuned for</li> </ul>	Ancich and Brown [3]
Insulation Below Joint Cavity	<400 Hz	<ul style="list-style-type: none"> <li>- Reduce noise coming from bottom of joint</li> <li>- Can block noise from wider range of frequencies than Helmholtz resonator</li> </ul>	<ul style="list-style-type: none"> <li>- Makes accessing underside of joint more difficult</li> </ul>	Mageba ROBO-MUTE
Concrete Enclosure of Joint Cavity (WSDOT Design)	<400 Hz	<ul style="list-style-type: none"> <li>- same strength as insulation below joint cavity</li> <li>- concrete has higher attenuation than insulating blanket</li> </ul>	<ul style="list-style-type: none"> <li>- retrofitting existing bridge with concrete could be difficult</li> </ul>	WSDOT design on SR520 bridge
Sinusoidal/Rhombus Plate	>400 Hz	<ul style="list-style-type: none"> <li>- Reduces noise radiating from top of the joint</li> <li>-reduces noise created by car tires running over joint gaps</li> </ul>	<ul style="list-style-type: none"> <li>- Retrofitting existing joints is difficult</li> <li>- Bolt-on, requires drilling into center beam. Increased corrosion risk</li> <li>- Road would need to be re-graded to account for increased height of joint</li> <li>- May limit mobility of joint</li> </ul>	Mageba Sinus Plate
Filling gaps between lamella beams	>400 Hz	<ul style="list-style-type: none"> <li>- When installed properly and in good condition, can reduce noise coming from top of joint</li> <li>- Easier than sinus plates to retrofit onto existing joints</li> </ul>	<ul style="list-style-type: none"> <li>- Durability is a concern</li> <li>- Has been tried on Golden Ears Bridge in Vancouver, BC, Canada. Reduces noise but increases maintenance required</li> </ul>	Ravshanovich et. al. [1]

### 3 Experiment Description

Measurement for this project were collected at two residential locations and at the SR520 bridge over five site visits between October 2018 and November 2018. An overview of the experimental site will first be presented followed by a discussion of existing noise abatement currently installed on the SR520 bridge. Finally, a description of the experiments in chronological order will be presented.

#### 3.1 Site Description

The Evergreen Point Floating Bridge (SR520 bridge) is a 2349.6 m (7708.5 ft) long floating bridge that spans Lake Washington and runs between the City of Seattle, WA on the west side and the City of Medina, WA on the east side. The floating portion of the bridge connects to shore by fixed approach bridges by way of short transition spans. Linking the transition spans to the floating bridge are large modular expansion joints built by Mageba. These large expansion joints are the focus of this study. It is bounded to the south by the Madison Park neighborhood of Seattle, to the North by Union Bay and the Laurelhurst neighborhood, and to the east by the City of Medina.

The westbound lane of the floating bridge includes shoulders with an inner width of 1.2 m (4 ft) and an outer width of 3 m (10 ft), two travel lanes and one high occupancy vehicle (HOV) lane. On the eastern end of the bridge, the HOV lane starts as two individual lanes that merge into a single lane just past the large expansion joint. Bicycles and pedestrians can access the bridge by a 4.3 m (14 ft) shared use path is located adjacent to the westbound lane. The eastbound lane of the floating bridge includes shoulders with the same dimension as the westbound lane, and two standard travel lanes. The eastbound lane on the east and west ends includes only a single HOV lane. All of the large expansion joints on the SR520 include 16 center (or lamella) beams. Small, seven center-beam expansion joints are also located on the west side of the bridge; several of which are installed with noise reducing sinus plates.



Figure 3-1: West-side measurement site (map from Google Earth)



Figure 3-2: East-side measurement site (map from Google Earth)

### 3.2 Existing Noise Abatement Measures

The design of the new bridge included three noise abatement features aimed at reducing the impact of noise on nearby residences; quieter pavement surfaces, noise walls, and the encapsulation of the underside of the large modular expansion joints.

To reduce the noise generated by cars driving over the bridge, grooved, noise-reducing pavements were installed on the bridge. These pavements have been shown to reduce road noise at frequencies above 630 Hz [8]. The quiet pavements on the bridge result in reduced road-traffic noise, which also lowers the overall ambient noise levels. As a result of these lower ambient noise levels, the noise generated by cars running over the modular expansion joints is more pronounced. Although previous noise studies have shown the new modular expansion joints to be quieter than those on the old bridge [9], the noise on the new bridge stands out more compared to ambient levels.

The noise walls are installed on the east side of the bridge on the north side of the westbound lane and on the south side of the eastbound lane. The walls start at Evergreen Point Road east on the approach bridge and terminate approximately 65 m (213 ft) from the large expansion joints on the east end of the bridge. The noise walls include several small breaks to accommodate small expansion joints on the approach bridge and transition span. As the walls end before the large modular expansion joints, they do not provide shielding from the expansion joint noise for residences adjacent to Lake Washington.

The cavities below the large modular expansion joints are fully enclosed below and on the water-facing side (west side of the cavity for east-side joints and east side of the cavity for the west side joints) however the land-facing side of the joint cavity (east side of the cavity for east-side joints and west side of the cavity for the west side joints) is partially open to allow for unrestricted bridge motion. This is an original design by WSDOT for the SR 520 ridge aimed at noise control.

### 3.3 Residential Measurements October 18, 2018

The first set of measurements were collected on October 18, 2018 at two residential locations in Medina, WA; 2839 Evergreen Point Road and 3221 Evergreen Point Road. Throughout these measurements wind speed was negligible and sky conditions were mostly sunny. 2839 Evergreen Point Road is located south of the large modular expansion joints on the east side of the bridge. Measurements were collected on the Brüel and Kjaer 2270 SLM from the west side of the property on the back porch of the house. The SLM was setup 3 m (9.8 ft) from the house with a receiver height of 1.5 m (4.9 ft). The direct line of sight between the bridge and the receivers was blocked by trees, however the noise from the cars running over the large expansion joints was still clearly audible. Data were collected between 9:50 am and 10:00 am. Over the course of the measurement, the noise from the joint increased and became more noticeable. This is potentially due to an increase in travel speed due to decreasing traffic volume.

The second site, 3221 Evergreen Point Road, is located just north of the large modular expansion joints on the east side of the bridge. Similar to the first site, the Brüel and Kjaer 2270 SLM was setup on the west side of the property approximately 15 m (49 ft) from the back of the hose. Unlike the first property, the second location had direct line of sight to the bridge with a short, 1.5 m (4.9 ft) hedge providing limited shielding. The receiver height was increased to 1.7 m (5.6 ft) so the microphone would be above the hedge. Data were collected between 10:48 am and 11:02 am.

### 3.4 Bridge Measurements

#### 3.4.1 East Side Joint Measurements October 23, 2018

On October 23, 2018 measurements were collected from the pedestrian walkway adjacent to the large modular expansion joint on the east end of the bridge. Data were collected using the Brüel and Kjaer 2270 SLM with a receiver height of 1.5 m (4.9 ft). During these recordings a Go-Pro camera was used to collect video of the car-pass events. Data were collected between 11:06 am and 11:12 am during which conditions were mostly cloudy with wind gusts up to but not exceeding 4.5 m/s (10 mph).

#### 3.4.2 West Side Joint Measurements November 1, 2018

On November 1, 2018 measurements were collected from the pedestrian walkway adjacent to the large modular expansion joint on the west end of the bridge. Data were collected using the Brüel and Kjaer 2270 SLM with a receiver height of 1.5 m (4.9 ft). During these recordings a Go-Pro camera was used to collect video of the car-pass events. Data were collected between 10:40 am and 10:46 am during which conditions were mostly cloudy with wind gusts up to 5.8 m/s (13 mph). Wind speed was recorded throughout the measurement and data where wind speeds exceeded 4.5 m/s (10 mph) were not included in the post-measurement analysis. Although it was not raining while data were collected the roadway was wet during the experiment and water was observed to be pooling between the joint on top of the waterproof seals.

#### 3.4.3 East Side Joint Measurements November 7, 2018

Measurements of the east side joint were collected on November 7, 2018 with the help of WSDOT. Data were collected on two microphones using the 2-channel feature of the Brüel and Kjaer 2270 SLM starting at 10:14 am. Data were recorded for the following microphone configurations;

- Measurements from the pedestrian walkway, east and west of the large expansion joint at a distance of 24 m (79 ft) and receiver height of 1.5 m (4.9 ft). Channel 1 was positioned on the west side and Channel 2 on the east side.
- Measurements from the pedestrian walkway, east and west of the large expansion joint at a distance of 24 m (79 ft) and receiver height of 0.6 m (2.0 ft) so the microphone is

shielded from the joint by the concrete barrier. Channel 1 was positioned on the west side and Channel 2 on the east side.

- Simultaneous measurements from the road deck and in the cavity below the expansion joint. Channel 2 was positioned on the road deck next to the barrier separating the pedestrian walkway from the travel lanes with a receiver height of 1.5 m (4.9 ft). Channel 1 was positioned in the joint cavity, 11 m (36 ft) from the sentinel structure and a receiver height of 1.5 m (4.9 ft).

For all measurement configurations, Go-Pro camera video recordings were collected to assist with post measurement analysis.

#### 3.4.4 West Side Joint Measurements November 8, 2018

Measurements of the west side joint were collected on November 8, 2018 with the help of WSDOT. Conditions on this day were foggy in the morning progressing to clear sky later in the day. Winds were negligible during the measurements. Data were collected on two microphones using the 2-channel feature of the Brüel and Kjaer 2270 SLM starting at 10:02 am. Data were recorded for the following microphone configurations;

- Measurements from the pedestrian walkway, east and west of the large expansion joint at a distance of 10 m (33 ft) and receiver height of 1.5 m (4.9 ft). Channel 1 was positioned on the west side and Channel 2 on the east side.
- Measurements from the pedestrian walkway, east and west of the large expansion joint at a distance of 20 m (66 ft) and receiver height of 1.5 m (4.9 ft). Channel 1 was positioned on the west side and Channel 2 on the east side.
- Simultaneous measurements from the road deck and in the cavity below the expansion joint. Channel 2 was positioned on the road deck with a receiver height of 1.5 m (4.9 ft) next to the barrier separating the pedestrian walkway from the travel lanes. Channel 1 was positioned in the joint cavity, 8 m (26 ft) from the sentinel structure and a receiver height of 1.5 m (4.9 ft).
- Measurements 3 m (10 ft) below the road deck 8 m (26 ft) east and west of the large joint to compare noise from the closed side of the joint cavity (east) and the side with openings (west) to see if leakage from the joint cavity occurs. Channel 1 was positioned on the west side and Channel 2 on the east side.

An additional measurement was also taken at a small expansion joint on the west approach bridge where sinus plates are installed. Measurements were collected using a single channel on the Brüel and Kjaer 2270 SLM. On the approach bridge the concrete barrier separating the pedestrian walkway and vehicle traffic are taller than those on then floating bridge. As a result, a receiver height of 1.8 m (5.9 ft) was used to prevent shielding by the concrete barrier.

## 4 Methodology

### 4.1 Equipment Description

Measurements were collected using a state of the art Brüel and Kjaer Type 2270-S, class 1 (BK2270) sound level meter (SLM). Acoustic data were recorded on either one or two channels at a sampling frequency of 48000 samples/s as 24-bit .wav files. Two free-field, half-inch, pre-polarized, omni-directional microphones were used; a Brüel and Kjaer Type 4189 with a flat response between 5 Hz and 20 kHz and Type 4966 with a flat response between 6.3 Hz and 20 kHz. Each microphone is attached to a Brüel and Kjaer Type ZC0032 preamplifier. To reduce wind-related noise one of two windscreens was used; a Brüel and Kjaer Type UA-1650 and Type UA-0237. For consistency, the UA-1650 windscreen is paired with the Type 4189 microphone and the UA-0237 windscreen is paired with the Type 4966 microphone. When the windscreens are used, the windscreen correction setting on the BK2270 is applied. The free-field setting on the BK2270 is also used throughout the measurements.

The .wav file output from the BK2270 are calibrated using a Brüel and Kjaer Type 4231 sound calibrator that generates a 1000 Hz calibration tone at  $94 \pm 0.2$  dB re  $20 \mu\text{Pa}$ . Before each measurement, a 90 s calibration tone was recorded. This was used to compute a receiving sensitivity,  $RS$ , for each microphone given by

$$RS = \frac{P_{cal}}{S_{rms}} \quad (3)$$

Where  $P_{cal}$  is the calibration pressure of 94 dB re  $20 \mu\text{Pa}$  (equivalent to a pressure measurement of 1.002 Pa) and  $S_{rms}$  is the root-mean-square of the calibration signal

$$S_{rms} = \sqrt{\frac{1}{N} \sum_{n=1}^N s_n^2} \quad (4)$$

Where  $s_n$  is the recorded value at time sample  $n$ , and  $N$  is the total number of samples in the recording. The calibration is applied as follows;

$$p_n = s_n \times RS, \quad n = 1, 2, \dots, N \quad (5)$$

Where  $p_n$  is the calibrated value at time sample  $n$ .

## 4.2 Data Processing

Identifying the time period when cars are passing over the expansion joints is the first step in processing these data. The car pass events are labeled using Audacity, an open source digital audio editor. The label feature in the program allows the start and end time of each individual event to be identified. In conjunction with video recordings taken during the measurement, this tool helped with identifying additional meta-data associated with each car pass event. This included car type, lane of travel, make/model and tire width (identified using make and model information).

Having identified each individual car-pass event in the data, the associated spectra for each event was computed. Due to the non-stationary and transient nature (varying time intervals and varying characteristics in time) of the noise, the energy spectral density (ESD) is used to measure the spectrum of each event [7], [10]. This is computed by first computing the power spectral density (PSD) using the periodogram function in the *scipy.signal* toolbox [11] in Python. This is then multiplied by the total duration of the event,  $T_e$ , and divided by the characteristic impedance,  $\rho c$ , where  $\rho$  is the density in air (1.225 kg/m<sup>3</sup>) and  $c$  is the speed of sound in air (340 m/s)

$$ESD = \frac{PSD \times T_e}{\rho c} \quad (6)$$

The ESD will be presented in dB referenced to  $E_{ref}$  of 1 J/m<sup>2</sup>/Hz (or  $10 \log_{10}(ESD/E_{ref})$ ). When A-weighting is applied to the ESD, a correction that accounts for the relative loudness of sounds perceived by the human ear, the ESD will be presenting as dBA. For the ESD computation, a Tukey (tapered-cosine) window with 25% tapering is applied to the time series, and a Fast-Fourier Transform (FFT) zero padded to a length of  $4 \times f_s$  (or 192000 samples) is used. Using a standard FFT length will allow spectral averages to be computed. It is important to note that ESD should not be confused with a pressure level widely used for measuring environmental noise. In comparing the ESD of two events, however, a higher ESD corresponds to a higher noise level.

The Federal Highway Administration uses either 15 min or 1 hr equivalent sound levels,  $L_{eq}$ , and third-octave sound levels to measure compliance and noise abatement criteria. In this report the ESD is used as it allows transient events with varying durations to be compared. This is an effective tool to help investigate the mechanism(s) responsible for the expansion joint noise including their spectral characteristics which is one of the main goals in this report.

To explore the relation between tire width and maximum frequency in the ESD, a Savitzky-Golay filter (least-squares filter[12]) is used to reduce the noise in the ESD of a single car-pass event. The filter is applied to the data using the *savgol\_filter* function in the *scipy.signal* toolbox using a 5<sup>th</sup> order polynomial and window length of 1001 samples.



## 5 Results and Discussion

In this section, measurements of the noise produced by cars passing over the expansion joints will be examined. First, measurements collected at two residential locations will be presented to determine the frequency content of the noise and how the noise at different locations compare. Measurements collected at the expansion joints are then examined to understand the character of the noise directly at the source, the origin of this noise (above or below the expansion joint) and any directional characteristics.

To better understand the noise generated by cars passing over the expansion joints, simultaneous noise and video recordings were collected from the pedestrian walkway at the large expansion joint on the east end of the bridge (Figure 5-1). The process of the car passing over the expansion joint, herein referred to as a vehicle-pass event or simply event, begins when the front tires of a vehicle passes from the transition span onto the modular expansion joint. The simultaneous video and noise recordings demonstrate that the noise level abruptly increases as this occurs. The noise level remains elevated until the front tires pass from the expansion joint onto the floating bridge. There is then a brief reduction in noise as the front wheels leave the expansion joint. For axel spacings that are shorter than the length of the modular expansion joint, this short reduction in noise levels is not observed. The noise levels then increase again as the rear wheels begins passing over the joint. Just west of the east side large expansion joint (or just east of the west-side large expansion joint) is a small, single-gap expansion joint. A small and brief increase in the noise levels is observed as the front and rear wheels pass over it. However, the noise from the large modular expansion joint is the dominant noise source and is therefore the focus of this study.

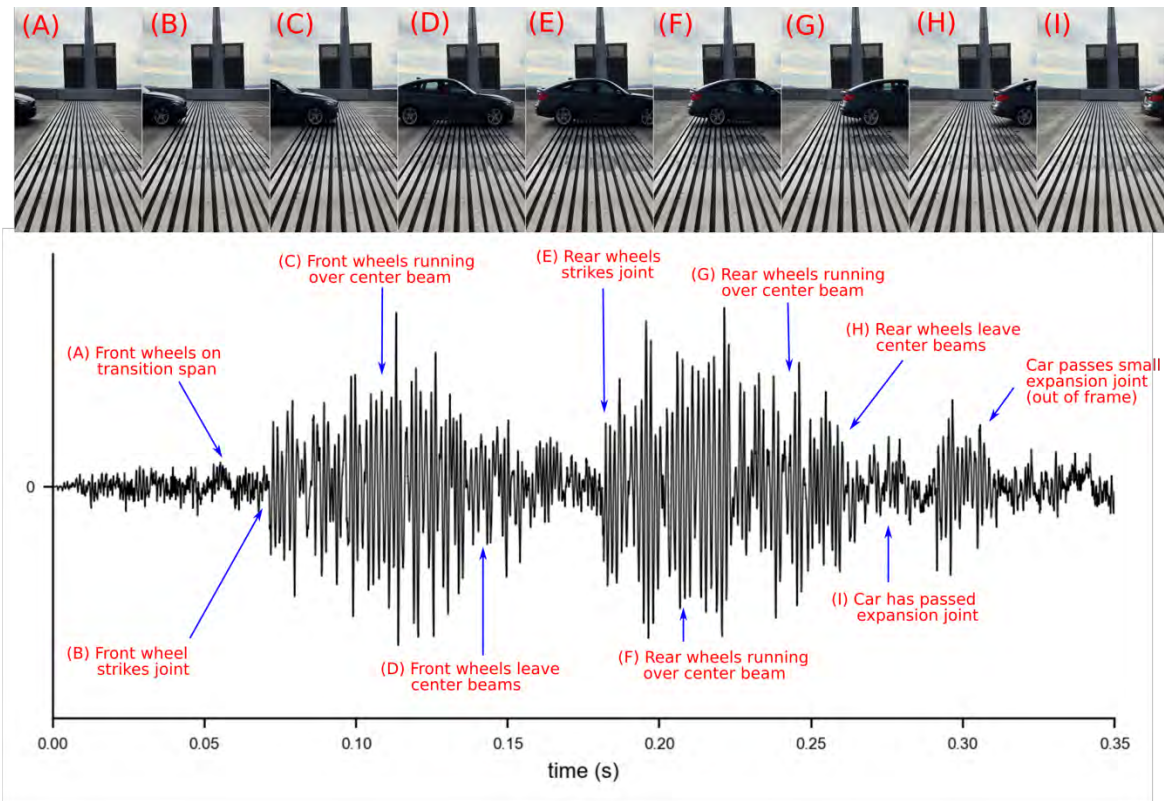


Figure 5-1: Overview of car-pass events using simultaneous noise and video recordings. Screen-shots from the video are attributed to specific parts of the noise recording using letters (A)-(I).

## 5.1 Residential Locations

In this section the average ESD will be computed for the measurements collected at the two residential locations on October 18, 2018; 2839 Evergreen Point Road and 3221 Evergreen Point Road. The average ESD of vehicle-pass events recorded at 2839 Evergreen Point Road (Figure 5-3(a)), south of the large expansion joints on the east end of the floating bridge, show the noise is primarily composed of frequencies between 500 Hz and 700 Hz with a sharp peak at 600 Hz. The average ESD was computed from 106 vehicle-pass events collected over two 2-minute periods for a total of four minutes.

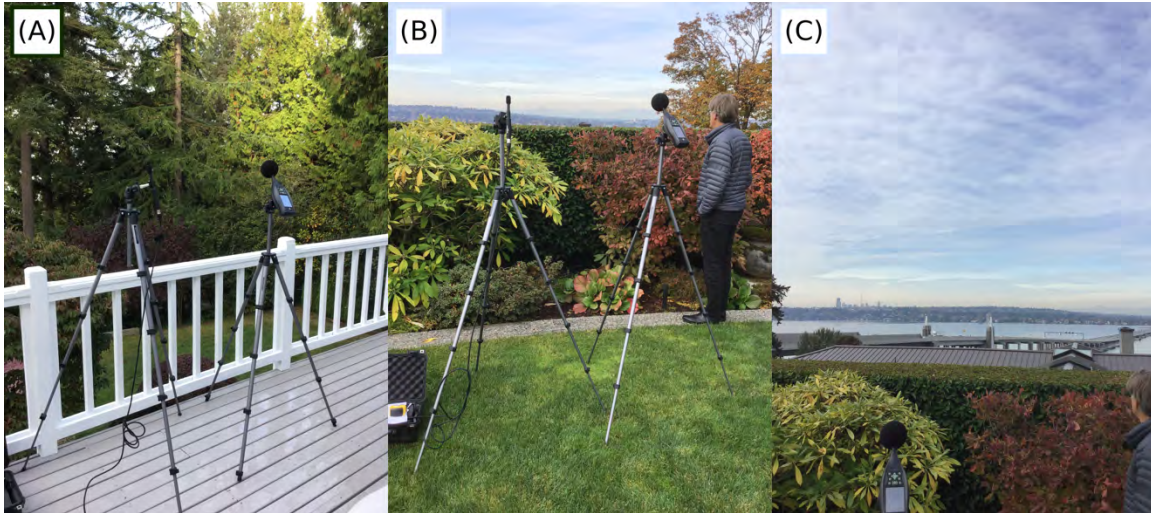


Figure 5-2: Equipment setup at (a) 2839 Evergreen Point Road, (B) 3221 Evergreen Point Road, and (C) view of expansion joint and sentinel on east side of bridge from 3221 Evergreen Point Road.

The ESD for 3221 Evergreen Point Road, north of the large expansion joints on the east end of the bridge, was computed from 66 car pass events collected over a consecutive four-minute period (Figure 5-3(b)). Similar to the first residential site, the average ESD shows the noise is characterized by frequencies above 500 Hz, however, unlike the first residential site where a 600 Hz peak can be observed, the second site exhibits high ESD between 500 Hz and 800 Hz.

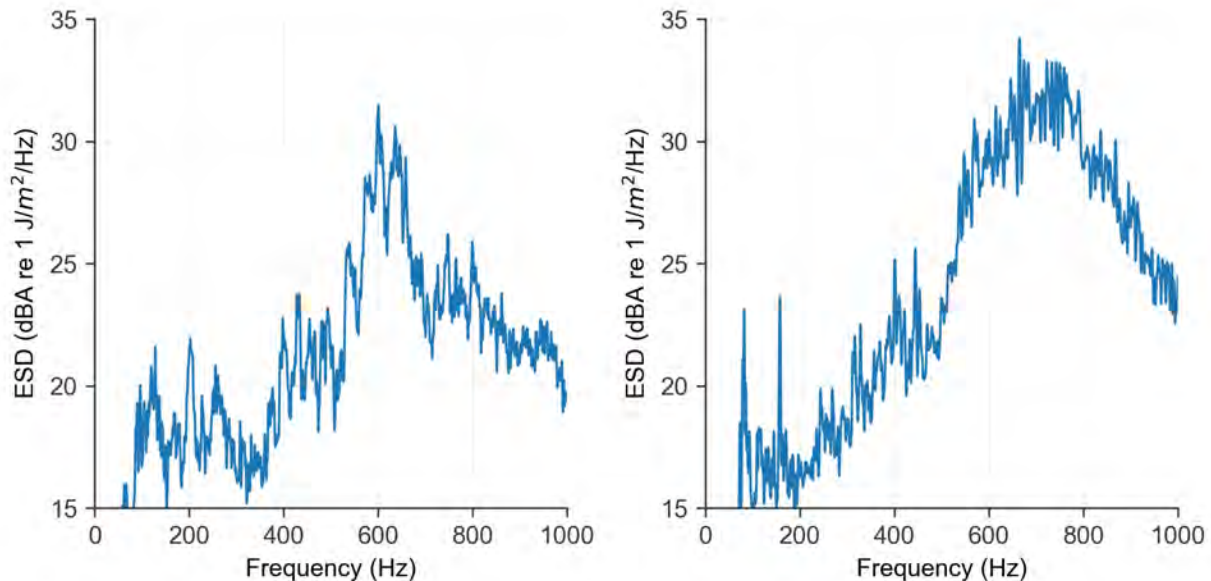


Figure 5-3: Average ESD of measurements collected at (a) 2839 Evergreen Point Road and (b) 3221 Evergreen Point Road

The differences in the ESD at the two residences is not immediately clear. One explanation could be due to lower traffic volumes when measurements were collected at 3221 Evergreen Point Road at 11:00 am compared to 10:00 am at 2839 Evergreen Point Road. Another possibility could be due to the direction of travel of vehicles on the closest expansion joint to the measurement

locations; 2839 Evergreen Point Road is closer to the large expansion joint on the east-bound lane where traffic moves towards the receiver whereas 3221 Evergreen Point Road is closer to the west-bound lane where traffic is moving away from the receiver. Another way of looking at this is measurements at 2839 Evergreen Point Road take measurements in front of the vehicles whereas measurements collected at 3221 Evergreen Point Road take measurements from behind the vehicle. It will be of interest to see whether the noise is directional; this will be explored further in Section 5.4.

## 5.2 Joint Measurements

Using the single channel measurements (Figure 5-4) collected at the east-side and west-side large expansion joints on the west-bound lane, the average ESD of car pass events are computed (Figure 5-5). The east-side measurements were collected on October 23, 2018 and November 7, 2018 with the ESD computed from a total of 293 vehicle-pass events and the west-side measurements were collected on November 1, 2018 and November 8, 2018 with the spectral average computed from a total of 376 vehicle-pass events.

The average ESD of the background noise levels (Figure 5-5) has also been computed for the east and west large expansion joints. To compute the background noise (which can include the noise from vehicles passing over the large expansion joint on the east-bound lane) the ESD was calculated for the 0.5 s time period before a vehicle passes over a joint and the 0.5 s period after the car has passed over the joint (Figure 5-6). From these data it is clear that the ESD from car pass events is well above the background levels, with the largest differences of up to 20 dB between 400 Hz and 800 Hz.

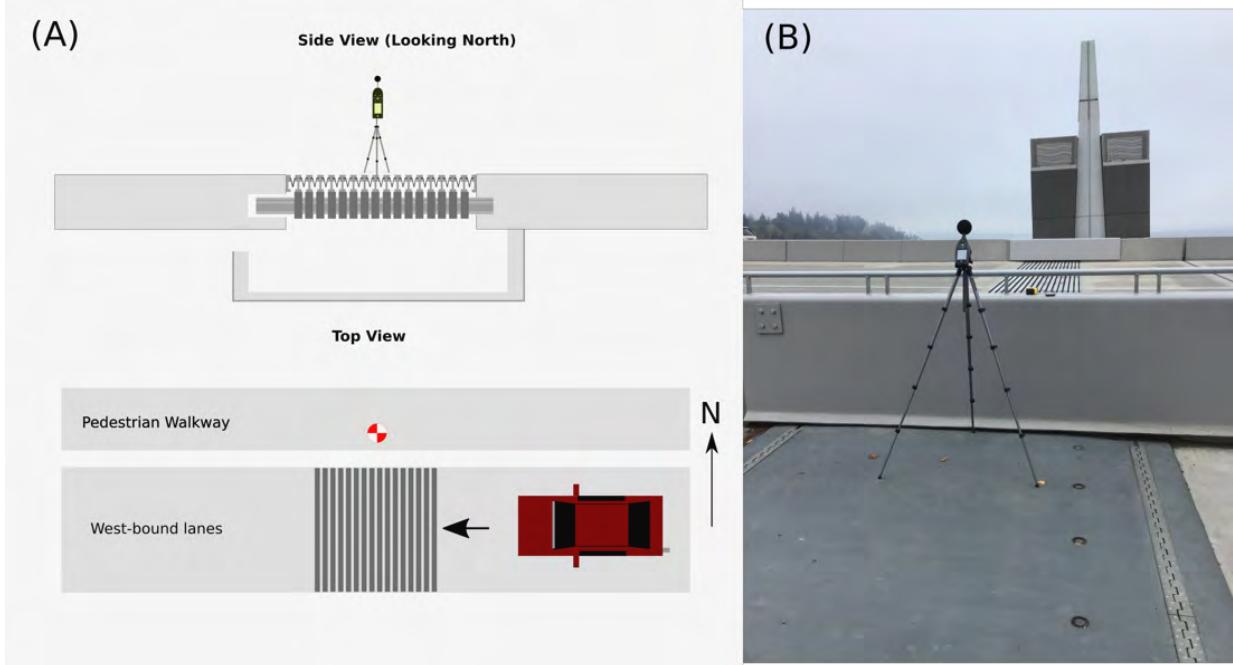


Figure 5-4: (A) Schematic of equipment setup for the single receiver measurements at the large expansion joints on the east and west sides of the bridge, and (B) Equipment setup at the large expansion joint on the east side of the floating bridge from the pedestrian walkway.

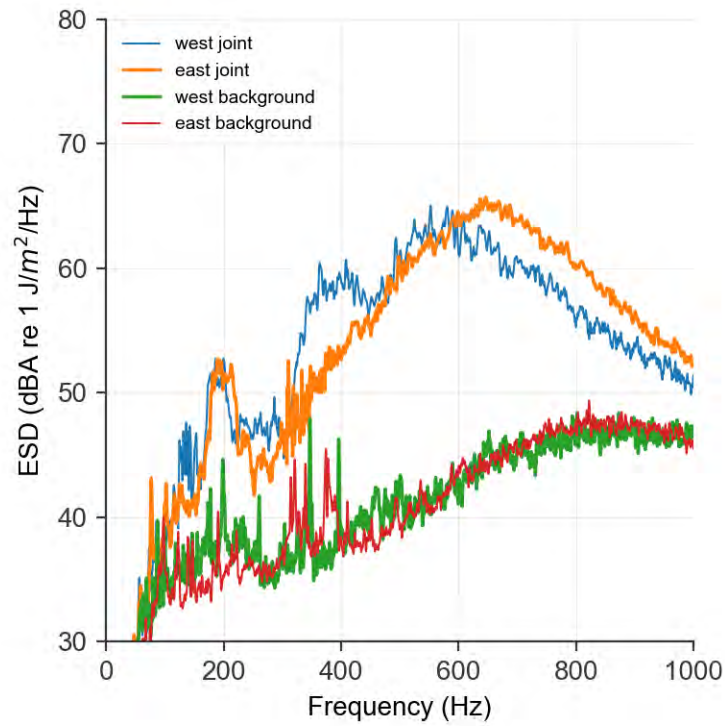


Figure 5-5: Spectral average of car pass events on October 23, 2018 and November 7, 2018 at the east side expansion joint (thick orange) and car pass events on November 1, 2018 and November 8, 2018 on the west-side expansion joint (thin blue line). The background levels are also shown for both expansion joints.

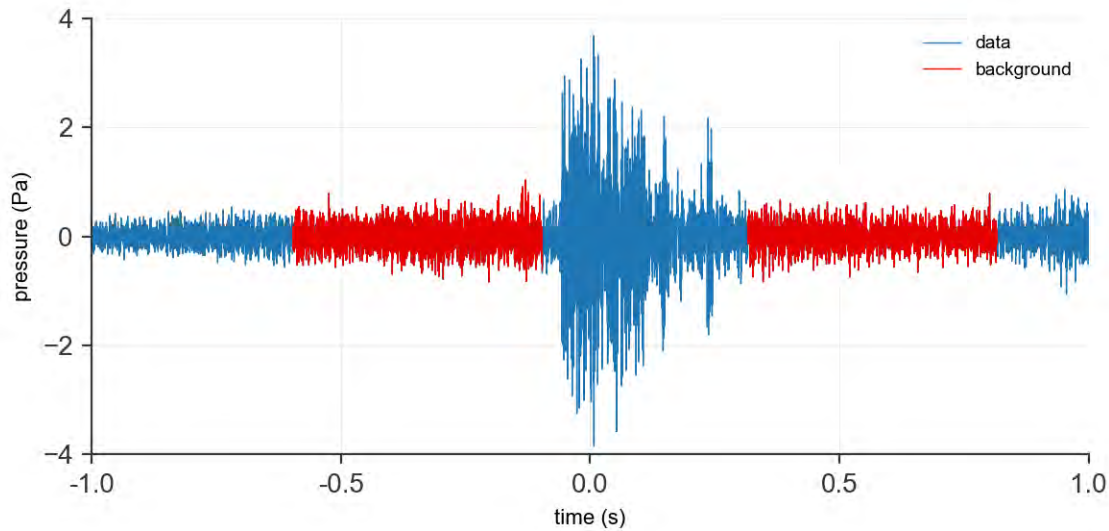


Figure 5-6: Time series (blue) of a single car-pass event centered at 0.0 s and the time samples used for calculating the ESD of the background noise (red)

The east-side large expansion joint shows the highest ESD between 500 Hz and 800 Hz with a maximum value at 600 Hz, similar to the residential measurements (Figure 5-3). The ESD from the east and west joint are similar up to 600 Hz however at higher frequencies the ESD for the west joint is lower. This could be a result of higher traffic volumes on the west joint (376 car pass events for the west joint and 293 events for the east joint) resulting in lower speeds.

For both measurements a secondary, local maximum is also observed at 200 Hz. The origin of this can be explored using the bar pass frequency,  $f_{bar}$  in Eq. (1). Assuming a vehicle velocity  $V$  of 26.8 m/s (60 mph), a center beam width  $W_b$  of 0.106 m (4 in) and a gap width  $W_g$  of 0.0381 m (1.5 in) gives a bar pass frequency of 192 Hz which is very close to the 200 Hz local maximum observed in Figure 5-5. Note that this local maximum is slightly below 200 Hz for the west joint whereas the local maximum for the east joint is slightly above 200 Hz. This gives further support to the hypothesis that traffic speeds were comparatively lower at the west-side joint. There is also a second local maximum for the west side joint at 400 Hz. This is potentially a harmonic of the bar pass frequency and why it only exists for the west joint is being investigated.

While the metrics and measurement protocols used in this report differ from those used in previous WSDOT studies [9], the overall characteristics of the third-octave measurements in both studies are consistent.

### 5.3 Measurements Above and Below Expansion Joint

In the previous section, measurements collected at the expansion joint showed high ESD between 400 Hz and 800 Hz, similar to the measurements collected at residential locations. The goal of this section is to determine if the majority of the noise heard at the residences emanate from the concrete joint cavity below the road deck or from the top of the expansion joint by comparing measurements collected above the expansion joint and in the joint cavity (Figure 5-7) and below the bridge on either side of the joint cavity (Figure 5-8).

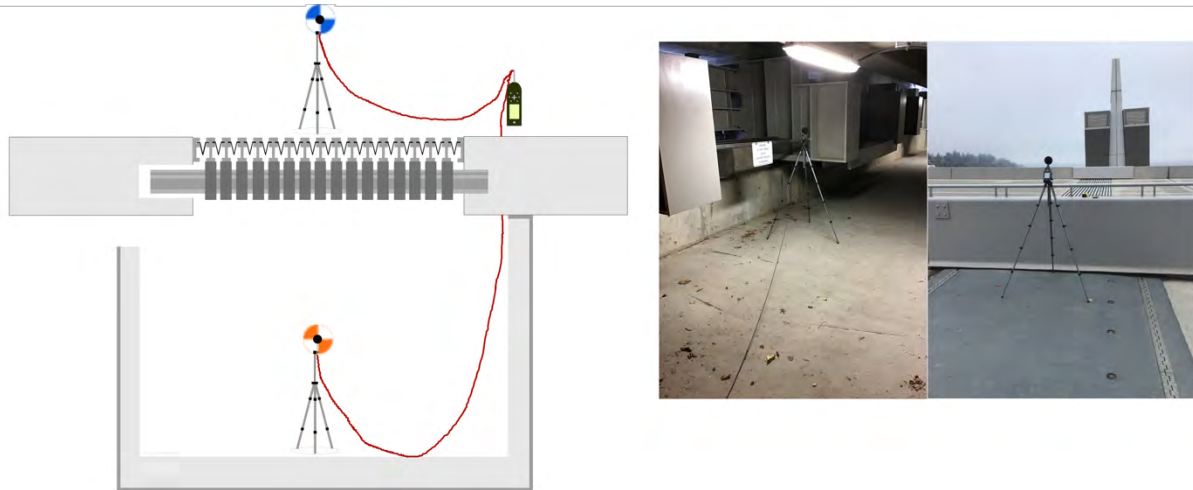


Figure 5-7: Equipment setup for simultaneous measurements collected above the expansion joint and in the joint cavity.

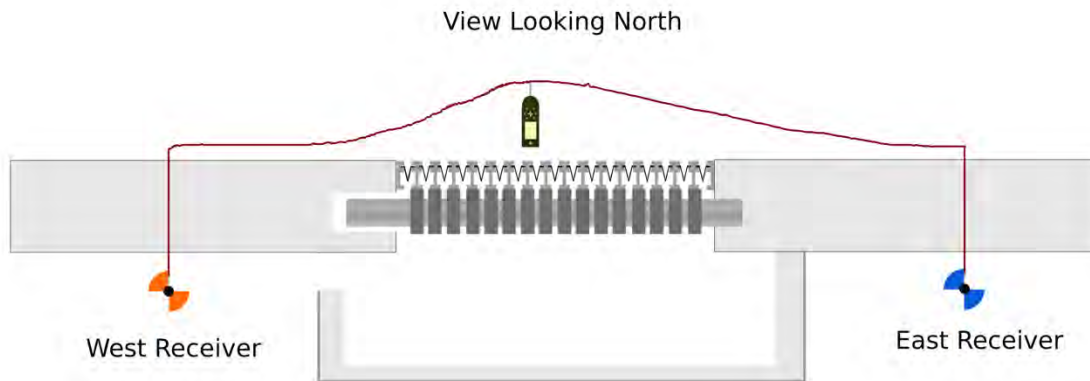


Figure 5-8: Equipment setup below the west-side large expansion joint with receivers east and west of the joint cavity.

The average ESD for measurements collected above the joint from the pedestrian walkway and below the joint in the joint cavity have been computed for the east joint using measurements collected on November 7, 2018 (Figure 5-9a) and for the west joint using measurements collected on November 8, 2018 (Figure 5-9b).

The results for joints (Figure 5-9a, b) exhibit the following trends;

- For frequencies over 300Hz the noise emanating from the top significantly dominates over the noise from the joint cavity
- The joint cavity amplifies the noise around 130Hz.
- Both the noise from the joint cavity and the top exhibit a peak at the shows a local maximum at the bar pass frequency of 190 Hz.

One explanation for the difference between the joint cavity measurements of the east side and west side expansions joints could be the location of the receiver in relation to the travel lanes on the road deck as they differed by 3 m with respect to the sentinel structures. Overall, it appears that the low frequency noise below 150 Hz originates in the joint cavity, around 200 Hz the noise above and below the joint have similar ESD, and above 350 Hz the noise originates from the top of the joint.

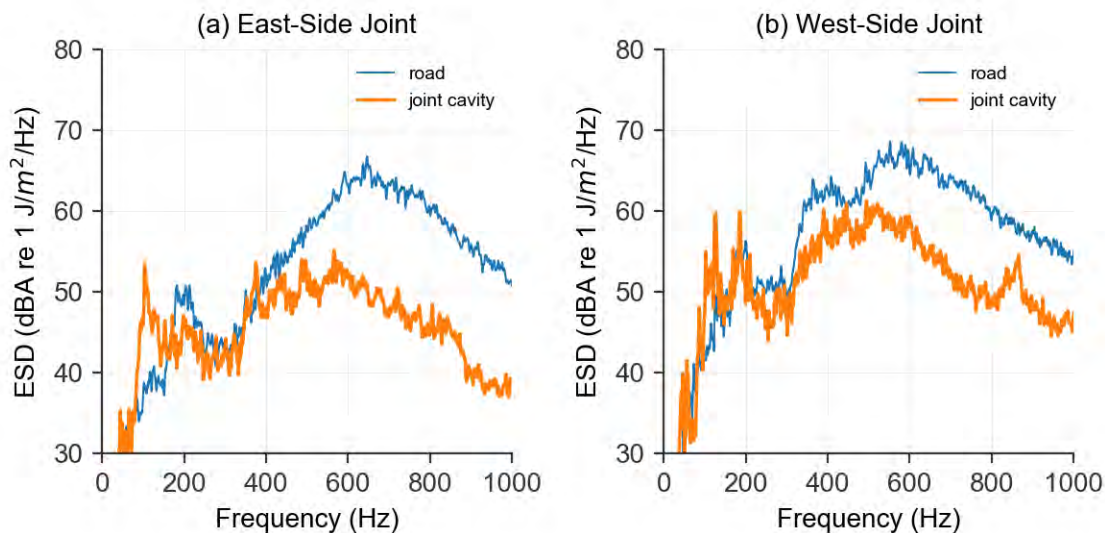


Figure 5-9: Comparison of ESD for noise measured above the joint and below in the joint cavity for the (a) east-side joint and (b) the west side joint.

The joint cavity is enclosed on the bottom and all sides except one, the side facing transition span connecting the floating bridge to the shore. To test whether noise travels out from the joint cavity, microphones were suspended 3 m below the west-side joint on either side of the joint cavity on November 8, 2018 (Figure 5-8). The results (Figure 5-10) show that the average ESD of the west side of the joint cavity (which has openings) is higher than the fully enclosed east side. The ESD from both receivers, however, are up to 15 dB lower than the ESD measured in the joint cavity and up to 25 dB lower than the ESD of vehicle-pass events measured on top of the bridge. The noise originating from the joint cavity therefore constitutes a marginal contribution to the overall noise received at the residential locations and further supports the fact that the majority of the noise radiates from the top of the joint.



The concrete enclosure is a unique feature designed by WSDOT specifically for the SR520 bridge. Comparing the noise in the joint cavity to the noise outside of the joint cavity (Figure 5-10) indicates that without this enclosure the noise originating on the underside of the bridge could contribute to the noise nuisance at low frequencies. Enclosing the underside of the joint, either by a concrete enclosure as was done for the SR520 bridge or using insulation (Mageba RoboMute™ or similar insulating material), should therefore be considered and is advised for other modular expansion joints on bridges near residential areas.

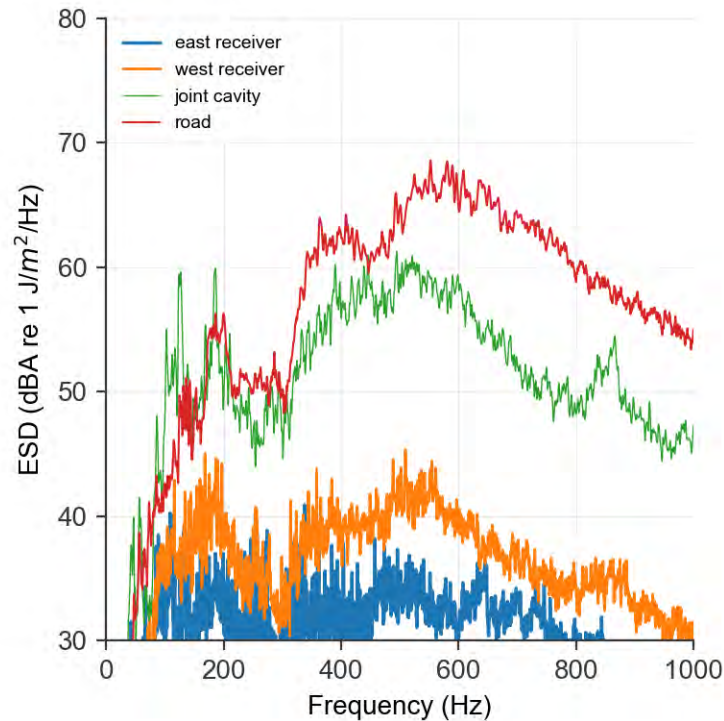


Figure 5-10: ESD of car-pass events measured below the west-side joint on the east and west side of the joint cavity. The west side of the joint cavity faces the transition span and has openings whereas the east side of the joint cavity is fully enclosed. These data are compared to the average ESD measured above the road and in the joint cavity.

#### 5.4 Directionality of Noise Above Joint

Qualitative observations were made during early site visits that the noise on one side of the joint was potentially louder than the other, indicating a directional-characteristic to the noise. To investigate this, two microphones were set up with one just east of the large expansion joints and the other just west. A spacing of 10 m and 20 m on the west-side expansion joint and a spacing of 24 m on the east-side large expansion joint (Figure 5-11) was used.

For the 10 m spacing on the west-side large expansion joints (Figure 5-12 (a)) the ESD obtained from the two microphones are very similar. Increasing the spacing to 20 m (Figure 5-12(b)) decreases the ESD peak of westbound noise with approximately 5 dB while the eastbound

(towards the residences) shows no significant decrease for frequencies higher than 400Hz. Below 400 Hz the west receiver exhibits similar results as the east receiver. By Increasing the distance to 24 m (Figure 5-12(c)) we see an even more pronounced difference between the east and west sides of the joint with differences in the ESD of up to 10 dB and higher. Road vehicle noise, in general, can exhibit directional characteristics but in this case the expansion joint noise is so much higher than traffic noise (based on background noise analysis in Figure 5-5) that the directional characteristics measured here can be attributed to the joint and not directional characteristics of the road or vehicle noise. One explanation is the front of the car provides shielding for the front receiver which would explain why receivers with small  $\theta$  show smaller differences.

Overall, these measurements indicate the noise produced above the joints displays directional characteristics with the receiver in front of the car exhibiting lower ESD than receivers behind the car. This difference between the two receivers increases as the angle  $\theta$  (Figure 5-11) between the car and receivers increases (Figure 5-11). This could lead to higher noise levels at residences that are closer to lanes of travel where traffic is moving away (e.g. 3221 Evergreen Point Road) whereas residences closer to lanes of travel where traffic is moving toward (e.g. 2839 Evergreen Point Road) could experience comparatively lower levels. This could explain why the ESD from 2839 Evergreen Point Way (Figure 5-3(a)) is lower than 3221 Evergreen Point Way (Figure 5-3(b)).

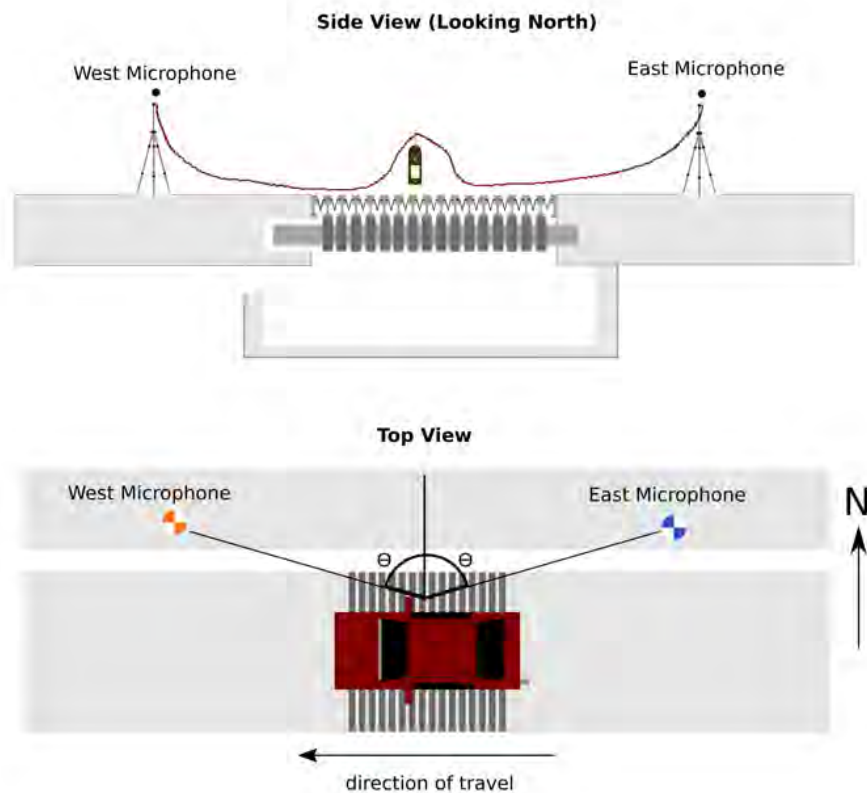


Figure 5-11: Equipment setup for measurements on the east and west side of the large modular expansion joints.

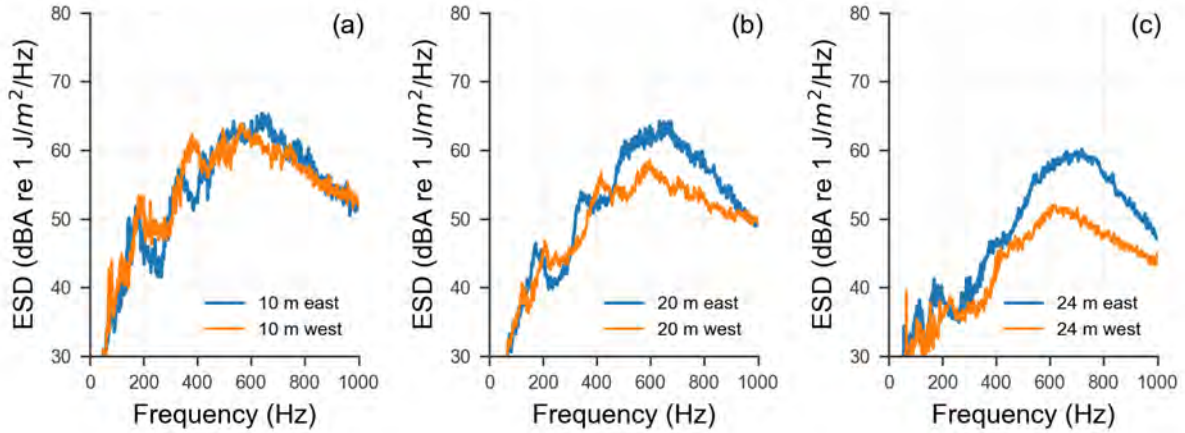


Figure 5-12: Measurements collected east and west of (a) the west-side large expansion joint with a receiver offset of 10 m, (b) the west-side large expansion joint with a receiver offset of 20 m, and (c) the east-side large expansion joint with a receiver offset of 24 m.

## 5.5 Tire Size Comparison

Having established the noise source originates on the top of the bridge, the next step is to determine the mechanism responsible for generating the noise. Based on a previous study by Ravshanovich et. al. [1], the relation between the tire width and center frequency is investigated. A range of events are compared to the resonance frequency determined by Eq.(2) using a sound speed  $c$  of 340 m/s and a characteristic length  $W$  determined by the tire width. Using video recordings to identify the make and model of vehicles passing the expansion joint, the tire widths are determined using manufacturer specifications. The actual tire widths can vary from manufacturer recommendations so verifying the precise tire widths is not possible. Manufacturer recommendations, however, are expected to provide reasonable estimates for the purposes of this study.

In previous sections, the variability of the data has been reduced by averaging the ESD from multiple car pass events (Figure 5-5 for example). Unfortunately, this approach cannot be used for this analysis as we are interested in discrete frequencies that are vehicle dependent. Instead, a Savitzky-Golay filter can be used to calculate a smoothed version of the ESD allowing a clearer comparison between the peak of the ESD and the resonance frequency from Eq.(2).

The results of the tire width analysis (Figure 5-13 with additional examples in Appendix A) show that the frequency with the highest ESD tends to be close to the resonance frequency predicted by Eq.(2); Figure 5-13(d) and Figure 5-13(f) are good examples of this relationship. The peak of the ESD does not, however, always fall within the expected range of the resonance frequency, and Figure 5-13(c) and Figure 5-13(e) demonstrate. Overall, however, the peak of the ESD,  $f_{peak}$ , does appear to be an inversely proportional to the tire width,  $W_t$ ,

$$f_{peak} \propto \frac{1}{W_t} \quad (7)$$

This gives further support to the hypothesis that the noise originates on the top of the joints (as opposed from the joint cavity below the joints) and is due to resonances excited in the air gap between the center beams.

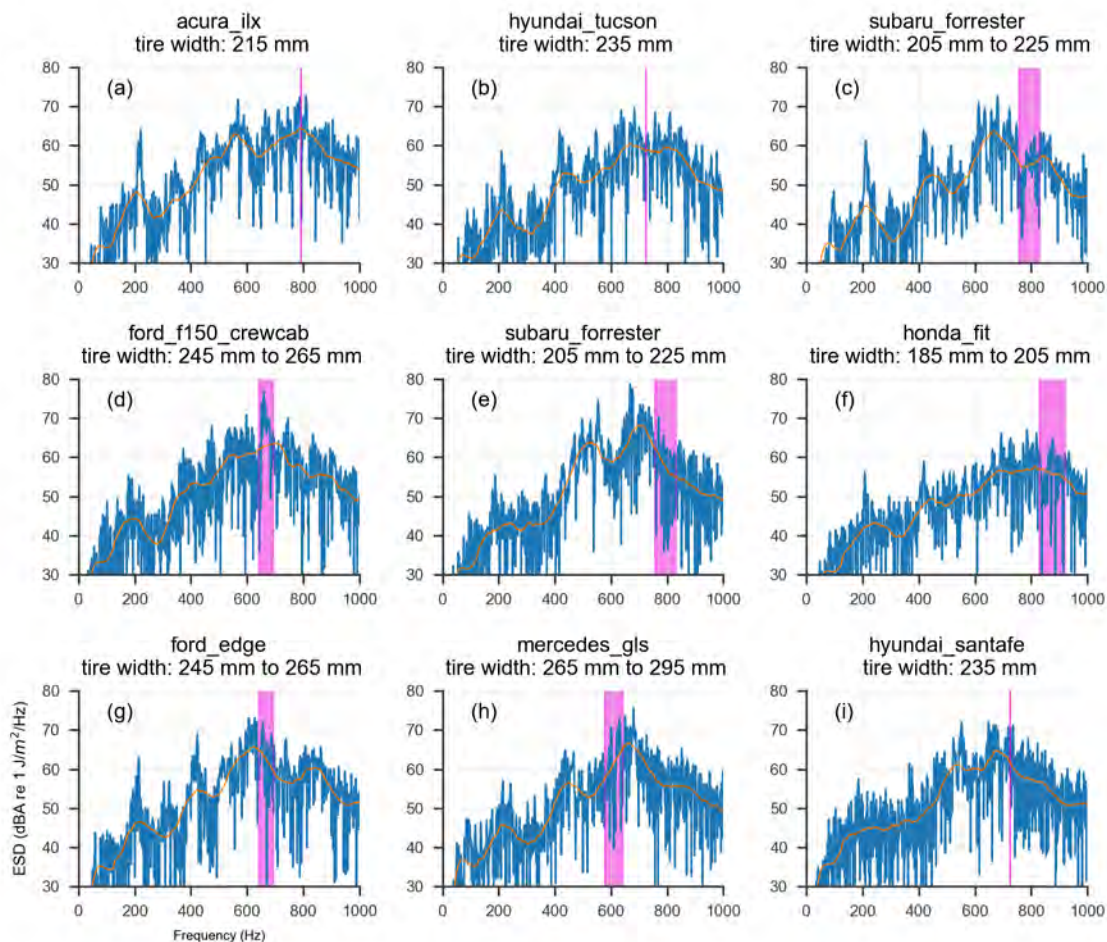


Figure 5-13: ESD of individual car-pass events (blue) compared to the resonance frequency associated with the car tire width. The resonance frequencies determined by Eq.(2) that are associated range of tire widths (highlighted in magenta) were identified using the minimum and maximum tire widths from manufacturer specifications of various body style and trim level. To provide a clearer relationship between the tire width and peak ESD, the broadband spectra have also been smoothed using a Savitzky-Golay filter (orange) to highlight the overall trend of the ESD.

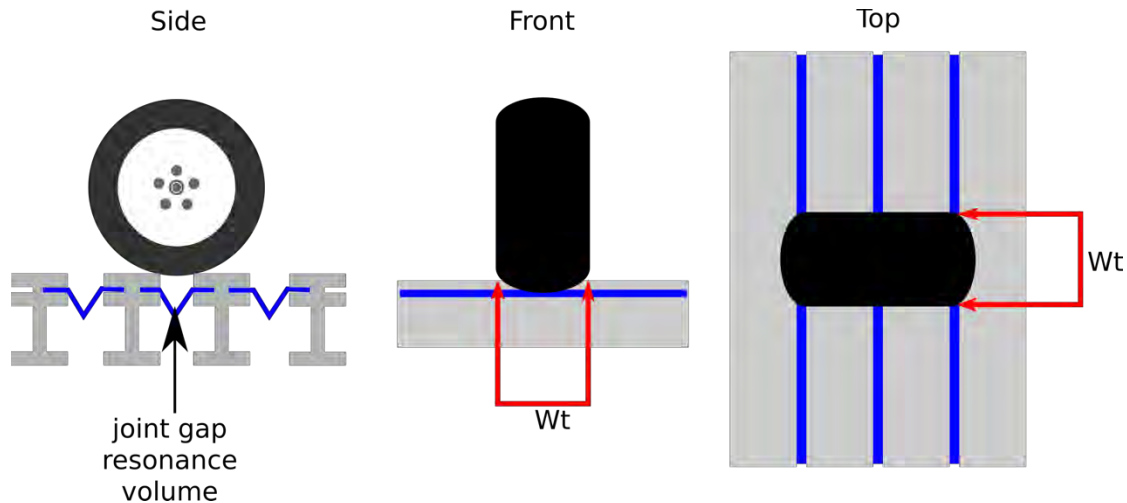


Figure 5-14: Volume formed by car tires rolling over gap between center beam. Resonance frequency determined by selecting  $L$  in Eq. (2) to be the width of the tire,  $Wt$ .

## 5.6 Sinus Plates

In this section the effect of sinus plates will be explored by comparing the average ESD of the small expansion joints with sinus plates to the large expansion joints on the east and west ends of the bridge. The sinus plate measurements were collected on the west approach bridge on November 8, 2018 (Figure 5-15). The ESD of the small joint with sinus plates is lower than the two large expansion joints, although it is important to note that explicit conclusions cannot be drawn from this comparison as the small joint with sinus plates has seven center-beams whereas the large expansion joints have sixteen. The ESD of large expansion joints are therefore expected to produce more energy overall during a vehicle-pass event than the smaller joint. The ESD of the small joint with sinus plates has a maximum value at approximately 600 Hz. This maximum has a sharper characteristic than the maximum of the two large expansion joints.

A better comparison uses the root-mean-square pressure ( $P_{rms}$ ) calculated using Eq. (4) with the pressure,  $P$ , used in place of the uncalibrated signal,  $S$ . The difference between  $P_{rms}$  of the large expansion joint and the small expansion joints with sinus plates is 5 dB indicating the sinus plates result in a reduction in noise levels. This is equal to the reduction reported by Mageba and is consistent with previous WSDOT measurements. Further study, however, is needed to determine whether the lower ESD for the small expansion joint is due to fewer center beams, the sinus plates, or some combination of the two. Measurements should be taken of identical joints with and without sinus plates installed for a direct comparison.

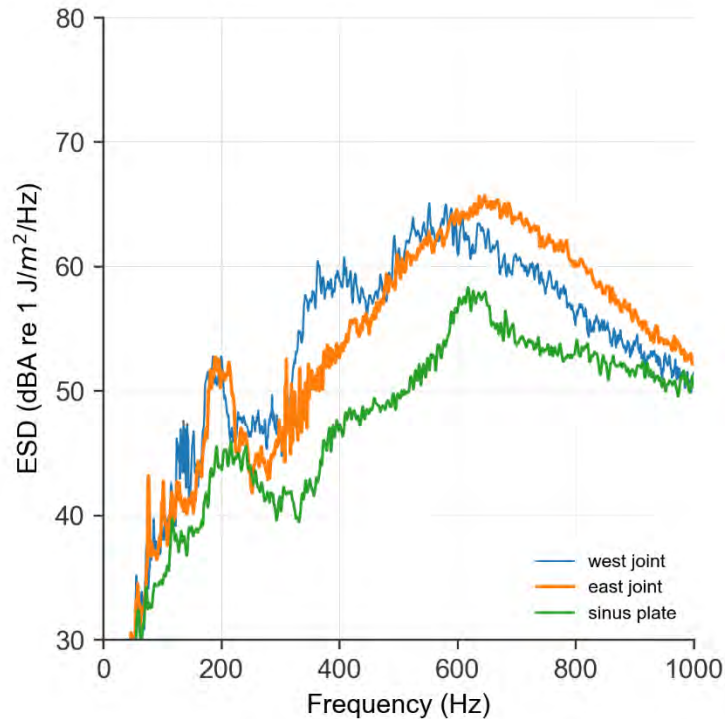


Figure 5-15: Average ESD of car pass events measured at the small expansion joint with sinus plates on the west approach bridge compared to large expansion joints on east and west sides of the floating bridge

## 5.7 High-Speed Camera Measurements

To understand the noise process by which vehicle tires generate noise, a high-speed camera was used to capture video recordings of the tires of different vehicles as they passed over the expansion joints. High-speed video recordings from four types of vehicles will be compared; sedan passages using recordings of a Toyota Prius (Figure 5-16) and Scion FR-S (Figure 5-17), SUV passages using a recording of a Toyota Tundra (Figure 5-19), heavy trucks using a recording of a car-carrier truck (Figure 5-20), busses using recordings from a King County Metro bus (Figure 5-21). The tire contact patch, or the portion of the tire that is in contact with the road, will be the primary focus in this section.

Comparing the two sedans (Toyota Prius in Figure 5-16 and Scion FR-S) appear to pass over the center-beams such that a single gap is covered, and the tire is in contact with the center beams on either side. The tire on the Toyota Prius appears to deform more compared to the Scion FR-S with the tire making almost full contact with center beams so the tire contact patch is larger. The Scion FR-S, however exhibits a smaller tire contact patch with little contact with the center beams as the tire passes over the gap.



*Figure 5-16 Frame from high-speed video recording of Toyota Prius front tire passing over east-side large expansion joint center beams.*



*Figure 5-17 Frame from high-speed video recording of a Scion sports car front tire passing over east-side large expansion joint center beams.*

Moving on to the SUV video recordings (unidentified SUV in Figure 5-18 and a Toyota Tundra Figure 5-19). The two recordings show similar results with the tire contact patch covering the gap and part of each center beam on each side of the gap. The contact with the center beams is less than the Toyota Prius (Figure 5-16) but more than the Scion FR-S( Figure 5-17).



*Figure 5-18 Frame from high-speed video recording of an SUV tire passing over east-side large expansion joint center beams.*



*Figure 5-19 Frame from high-speed video recording of a Toyota Tundra front tire passing over east-side large expansion joint center beams.*

Comparing the car-carrier truck (Figure 5-20) and a bus (Figure 5-21), the tire contact patch of both vehicles is large enough that two gaps are covered and contact is made with three center beams. Both tires are deformed at the point where they run over the middle center beam that they are in contact with. The bus tires appear to sink into the gaps whereas the car-carrier truck tires do not appear to deform such that they sink down into the gaps. This could impact the pressure changes within the gaps.





*Figure 5-20 Frame from high-speed video recording of a car-carrier truck front tire passing over east-side large expansion joint center beams.*



*Figure 5-21 Frame from high-speed video recording of a bus front tire passing over east-side large expansion joint center beams.*

The high-speed video recordings demonstrate how the tires of various vehicles run over the expansion joints and the variability in how the tire contacts the modular expansion joints. Mitigation options such as the sinus plates or filling the gaps between the center beam provide a flat surface for the tires to roll over. This may reduce the impact of the tire on the gap thereby reducing the resonance response.

The high-speed video can be compared to the average ESD of the four types of vehicles; sedans, SUVs, trucks, and busses (Figure 5-22). The average ESD was computed from 202 car events, 286 SUV events, 20 truck events, and 10 bus events. It appears that the larger tire patch length of the truck and busses (Figure 5-20 and Figure 5-21) correspond to higher ESD. In particular at 200 Hz, attributed to the bar-pass frequency given by Eq. (1), the truck and bus events are 10 to 15 dB

higher than the car and SUV events. This could be due to the greater weight of these vehicles compared to lighter cars and SUVs that result in greater impact forces.

A future study, if funded, could collect simultaneous noise and video recordings to better understand the relationship between the interaction of the tire and the expansion joint. A pressure sensor will also be placed within a joint gap during the recordings to understand how the pressure changes within the joint gap relate to the measured sound. Two variables that should be included in this study are the vehicle weight and the tread pattern as this may provide insight on the resulting acoustic energy produced.

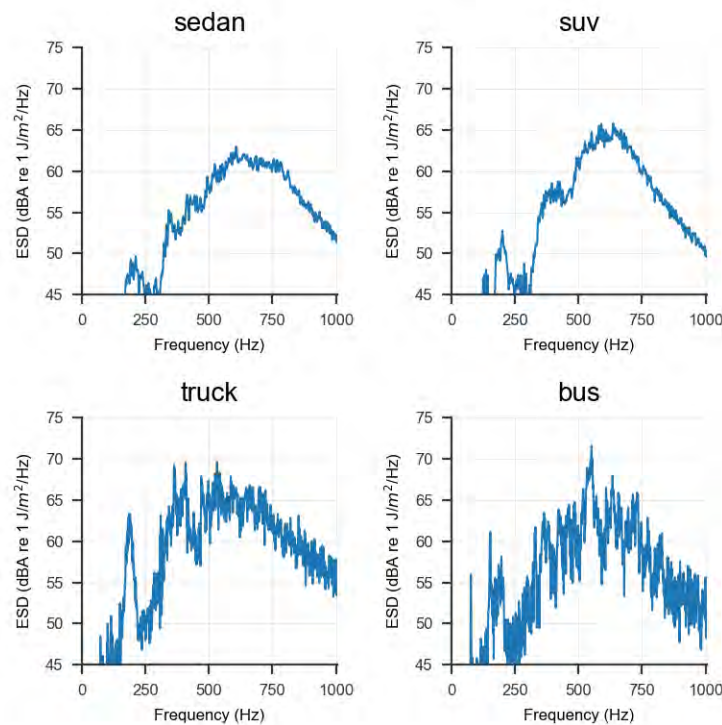


Figure 5-22: Average ESD for varying vehicle types (sedan, SUV, truck and bus) using data collected at the east-side large expansion joint on October 23, 2018 and November 7, 2018 and at the west-side large expansion joint on November 1, 2018 and November 8, 2018.

## 5.8 Noise Abatement Options

In this section the results of the SR520 bridge case study will be generalized and extended to address expansion joint noise in general. As discussed earlier, the mechanisms responsible for the noise can be divided into two categories; noise originating on the underside of the joint and noise from the top of the joint.

The noise originating below the bridge is characterized by low frequencies below 200 Hz. Three of the noise abatement options (Table 1) can address this; concrete enclosure of the joint cavity, insulating material to cover the joint cavity or Helmholtz resonators. Of the three options, enclosing the joint (a WSDOT design used on the SR520 bridge) is the best option as concrete has

a very high transmission loss. One design improvement for the concrete enclosure would be to have the opening face towards the center of the bridge instead of towards the shore and covered by a flexible sound barrier. The ESD from the open side (Figure 5-10) is higher than the closed face, although both are significantly lower than the ESD measured on the top of the joint and in the joint cavity. On existing bridges without noise abatement below the expansion it is difficult and expensive to add concrete enclosures so installation of a sound insulating blanket system could be the better option, although further testing and analysis of durability and maintenance costs would be needed to validate this assertion. The Helmholtz resonator could also be used on existing joints; however, this solution is more difficult to implement as it requires tuning the absorbers to the main joint resonance frequency.

The noise above the joints is characterized by frequencies between 400 Hz and 1000 Hz with the specific center frequency determined by the tire width. Three of the noise abatement options can address this mechanism; acoustic barriers, filling the center beam gaps or sinus plates. Noise barriers can be effective in certain situations, but there are serious limitations to their use. The range at which they are effective is limited and they cannot prevent refracted noise.

Sinus plates (or rhombus plates) potentially reduce the noise levels at the source as opposed to noise barriers which increase the transmission loss. Further study is needed to confirm their effectiveness in reducing noise levels. Manufacturers claim a 5 dB reduction which is equal to the difference in the RMS pressure of the large expansion joints and the small expansion joints with sinus plates. Further study is needed to independently confirm this. Additionally, installing sinus plates on existing joints can be difficult and further engineering analysis is needed to determine whether or not it is possible. Sinus plates may also limit the range of movement for large expansion joints in one or more directions. Therefore, additional engineering analysis is needed to determine whether sinus plates can allow for the large movements that floating bridge structures undergo and test how their installation on a floating bridge impacts longevity, safety and durability of the expansion joints.

Filling the gaps between expansion joints is also a viable option for reducing noise produced on top of the joints, particularly for existing structures or structures with complex movements such as floating bridges. This solution, which has been used in the Golden Ears Bridge in Vancouver, BC Canada, has significant durability issues and has to be regularly repaired. See Appendix B for a maintenance report from the bridge. Further study is therefore needed to select the best materials and test their durability. Additionally, the amount of noise reduction and how it is affected by the degradation of the filler material needs to be evaluated.

## 6 Summary and Recommendations

### 6.1 Summary and Recommendations for SR520 Bridge

1. The noise as evaluated by the energy spectral density (ESD) at residential locations is highest between 400 Hz and 800 Hz. ESD at the bridge close to the expansion joint is also highest between 400 Hz and 800 Hz.
2. The noise below the expansion joint is highest at frequencies below 200 Hz.
3. The noise above the expansion joints is highest at frequencies between 400 Hz and 800 Hz.
4. The majority of the noise at SR 520 bridge radiates from the top of the modular expansion.
5. Frequency characteristics of the noise for vehicle-pass events are closely related to vehicle tire width. The frequency peak for wider tires occurs at lower frequencies than for narrower tires. This is due to excitation of the air volume between the tire and the air gap between center beams.
6. Concrete joint cavity enclosure (WSDOT design) significantly reduces the noise coming from underside of bridge
7. A preliminary analysis suggests that sinus plates reduce noise levels between 400 Hz and 800 Hz by 5 dB. Further study is needed to confirm this.
8. Filling the gaps between the center beams or the installation of sinus plates are the two existing mitigation options that could reduce the noise on the SR520 bridge. More engineering analysis would be needed to determine whether sinus plates could be added to the large modular expansion joints on the floating bridge.
9. Based on the existing information, filling the gaps is the more viable option. Additional testing and research are needed to determine the effectiveness and durability of this approach.
10. The quieter pavement surfaces used reduced the overall background noise of the roadway which can provide masking for the noise from the expansion joints. This makes the expansion joint noise stand out from the background noise and be more pronounced.

### 6.2 General Conclusions for All Modular Expansion Joint

1. Low frequency noise (<400 Hz) comes from below the expansion joint. Bridges without enclosed joints could have substantial below-deck noise.
2. Noise radiating from below can be controlled with a concrete joint enclosure (as installed on SR 520 bridge) or insulating material installed on underside of the joint cavity.
3. The majority of energy of the noise radiating from the top of the expansion joints is between 400 Hz and 800 Hz.
4. Frequency characteristics of noise coming from the top of the expansion joint are closely related to the vehicle tire width (wider tires excite lower frequencies and narrower tires excite higher frequencies)

5. Best existing options for controlling noise between 400 and 800 Hz are either sinus plates or filling the joint gaps. For existing expansion joint, filling the gaps between the center beams is the better option.
6. Concrete enclosure or insulating materials are the best existing options for controlling noise radiating from the underside of the bridge.
7. Noise barriers can reduce noise levels at some residential locations but will not help residences farther away nor will they prevent refracted noise. According to WSDOT, the benefits of a noise barrier “decreases as a listener moves farther away and is negligible at distances greater than 500 feet” [13]. They can be beneficial in certain situations, but a proper analysis for each scenario is needed prior to installation.

### 6.3 General Recommendations

1. A controlled laboratory study would be valuable to both study the noise reduction from sinus plate installation and from filling the gaps between the center beams with foam.
2. A controlled study would also provide an opportunity to study the relationship between vehicle speed and the overall amplitude of the noise.
3. Additional work and laboratory testing to study filling the gaps between the center beams with a flexible material/structure. This includes the amount of noise reduction, the best material to use (most durable), installation best practices, and how degradation of the filler impacts the noise reduction.
4. Preliminary study of sinus plates shows a 5 dB reduction. Further study comparing joints of the same size (number of center beams) with and without sinus plates is needed for this to be confirmed.
5. Structural and corrosion analysis and laboratory testing is needed to determine whether sinus plates can be installed on existing expansion joints on floating bridges.
6. Sinus plate can limit the movements of expansion joints. Additional engineering analysis is needed to determine whether sinus plates can allow for the large movements that floating bridge structures undergo and test how their installation on a floating bridge impacts longevity, safety and durability of the expansion joints.<sup>4</sup>

## References

- [1] K. A. Ravshanovich, H. Yamaguchi, Y. Matsumoto, N. Tomida, and S. Uno, "Mechanism of noise generation from a modular expansion joint under vehicle passage," *Eng. Struct.*, vol. 29, no. 9, pp. 2206–2218, Sep. 2007.
- [2] E. J. Ancich and S. C. Brown, "Modular Bridge Joints – Reduction of noise emissions by use of Helmholtz Absorber," in *Fifth Austroads Bridge Conference*, Hobart, Tasmania, 2004, p. 12.
- [3] E. Ancich and S. Brown, "Engineering Methods of Noise Control for Modular Bridge Expansion Joints," *Acoust. Aust. Aust. Acoust. Soc.*, vol. 32, pp. 101–107, Dec. 2004.
- [4] J. P. Ghimire, Y. Matsumoto, and H. Yamaguchi, "Vibro-acoustic analysis of noise generation from a full scale model of modular bridge expansion joint," *Noise Control Eng. J.*, vol. 56, no. 6, p. 442, 2008.
- [5] J. P. Ghimire, Y. Matsumoto, H. Yamaguchi, and I. Kurahashi, "Numerical investigation of noise generation and radiation from an existing modular expansion joint between prestressed concrete bridges," *J. Sound Vib.*, vol. 328, no. 1, pp. 129–147, Nov. 2009.
- [6] I. L. Vér and L. L. Beranek, *Noise and Vibration Control Engineering: Principles and Applications: Second Edition*. John Wiley and Sons, 2007.
- [7] Malcolm J. Crocker, *Handbook of Noise and Vibration Control*. John Wiley & Sons, Inc., 2008.
- [8] J. L. Rochat and D. Reiter, "Highway Traffic Noise," *Acoustics Today*, vol. 12, no. 4, pp. 38–47, Winter-2018.
- [9] "SR 520 Floating Bridge and Landings Project: Joint Noise Recap, April 2016 - April 2017," WSDOT, May 2017.
- [10] T. D. Rossing, *Springer handbook of acoustics*. New York, N.Y.: Springer, 2007.
- [11] E. Jones, E. Oliphant, and P. Peterson, *SciPy: Open Source Scientific Tools for Python*. 2001.
- [12] W. H. Press, *Numerical recipes: the art of scientific computing*, 3rd ed. Cambridge, UK ; New York: Cambridge University Press, 2007.
- [13] "Road noise and noise walls - WSDOT." [Online]. Available: <https://www.wsdot.wa.gov/environment/protecting/noise-walls>. [Accessed: 07-Jan-2019].

## Appendix A. Tire Width Study

The make, model, range of tire widths from manufacturer specifications and lane of travel have been identified from video recordings for a 112 car pass events on October 23, 2018. The figures below include the ESD for each car pass event (blue), the ESD smoothed using a Savitzky-Golay filter (orange), and the resonance frequency from Eq. (2) for the range of tire widths. The sound speed,  $c$ , in Eq. (2) is approximated to 340 m/s.

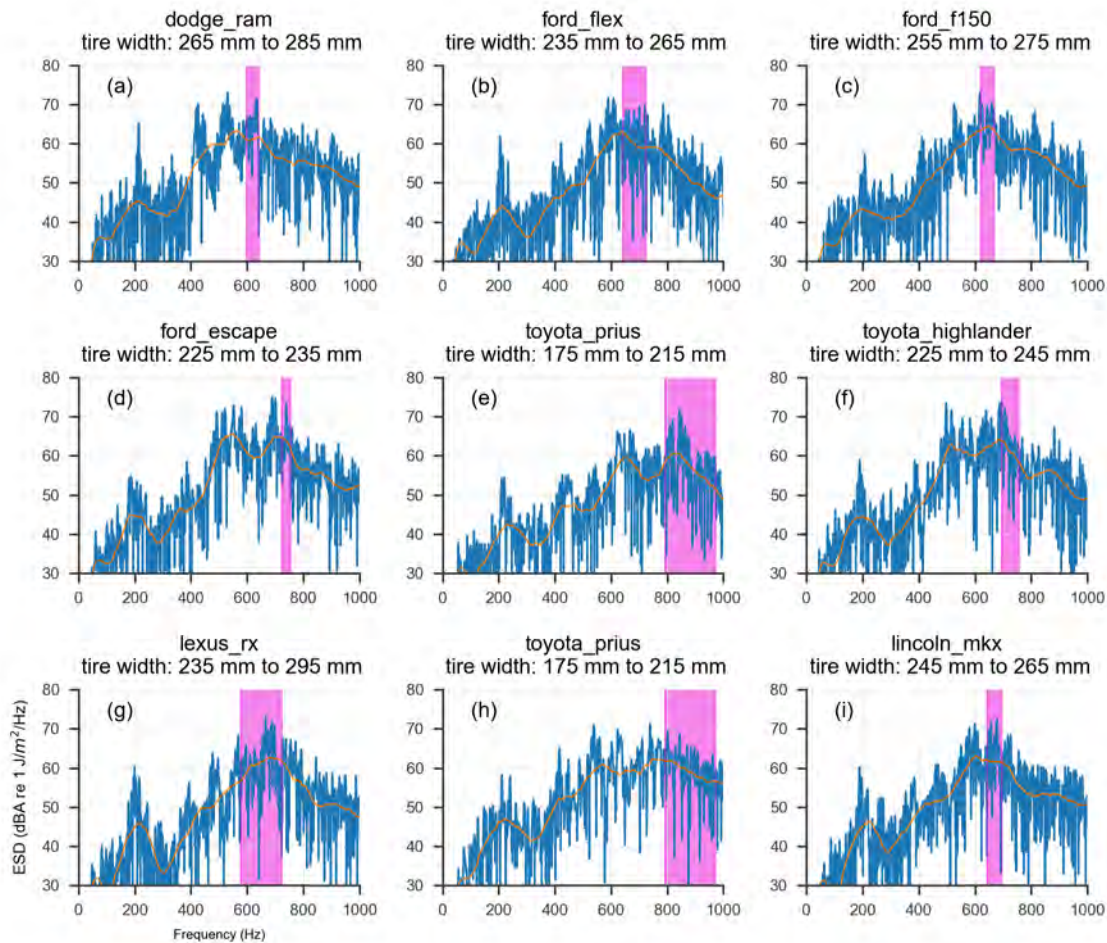


Figure A-1: ESD of car pass events (blue) and ESD with Savitsky-Golay smoothing filter (orange) compared to resonance frequency calculated using Eq. (2).

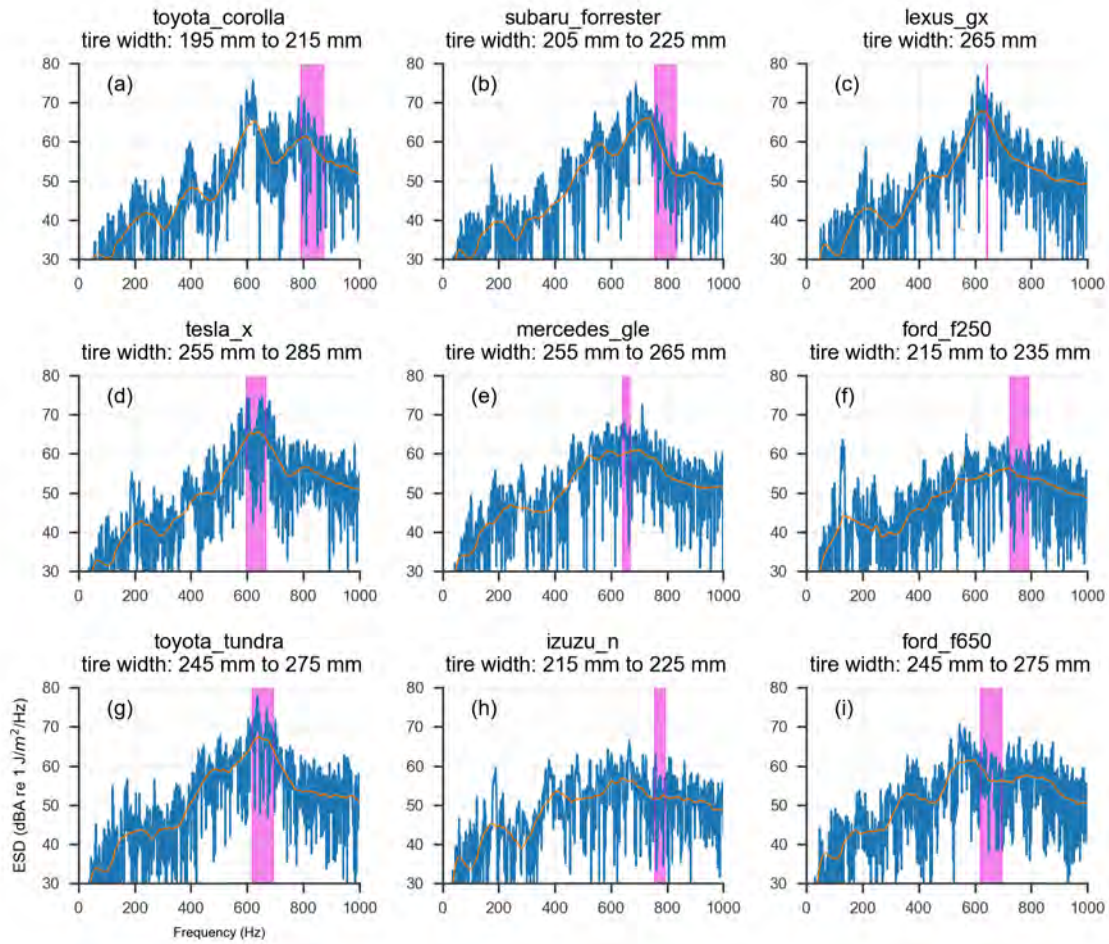


Figure A-2: ESD of car pass events (blue) and ESD with Savitsky-Golay smoothing filter (orange) compared to resonance frequency calculated using Eq. (2)



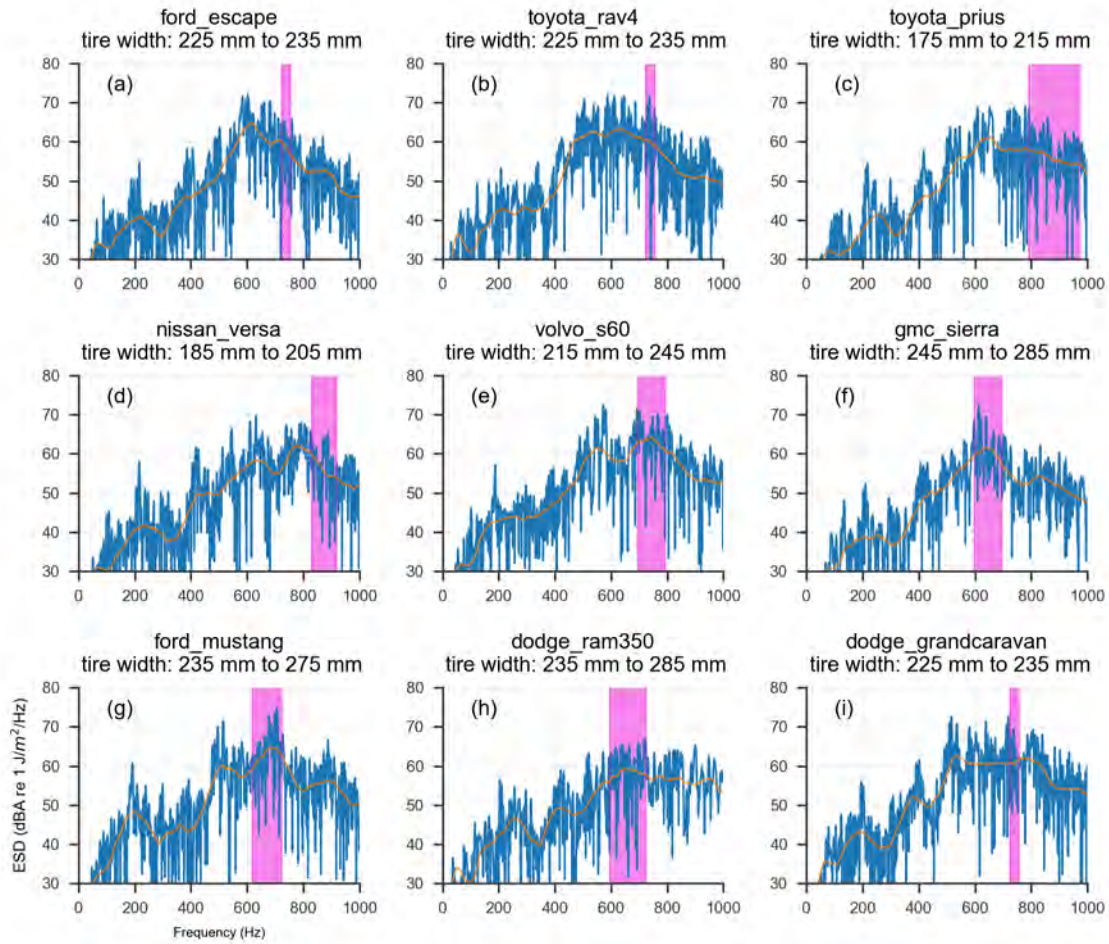


Figure A-3: ESD of car pass events (blue) and ESD with Savitsky-Golay smoothing filter (orange) compared to resonance frequency calculated using Eq. (2)

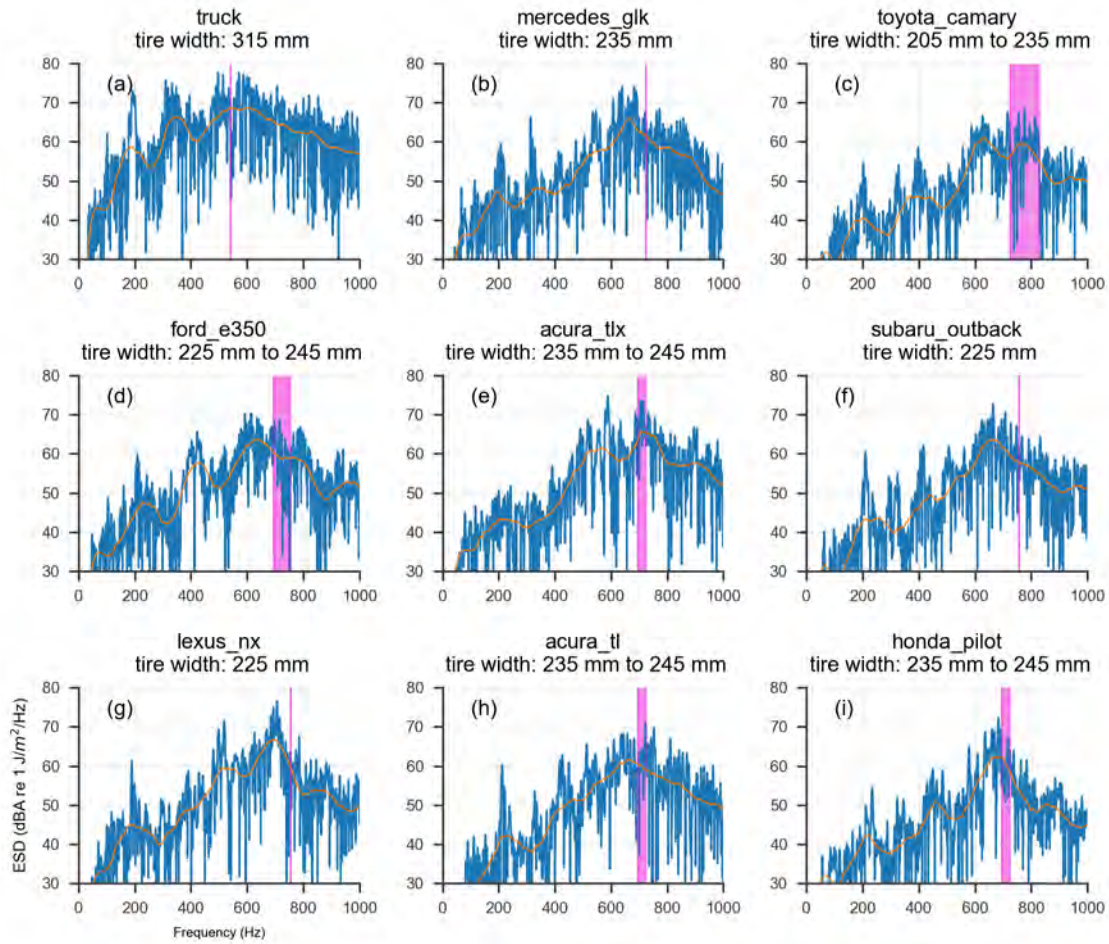


Figure A-4: ESD of car pass events (blue) and ESD with Savitsky-Golay smoothing filter (orange) compared to resonance frequency calculated using Eq. (2)

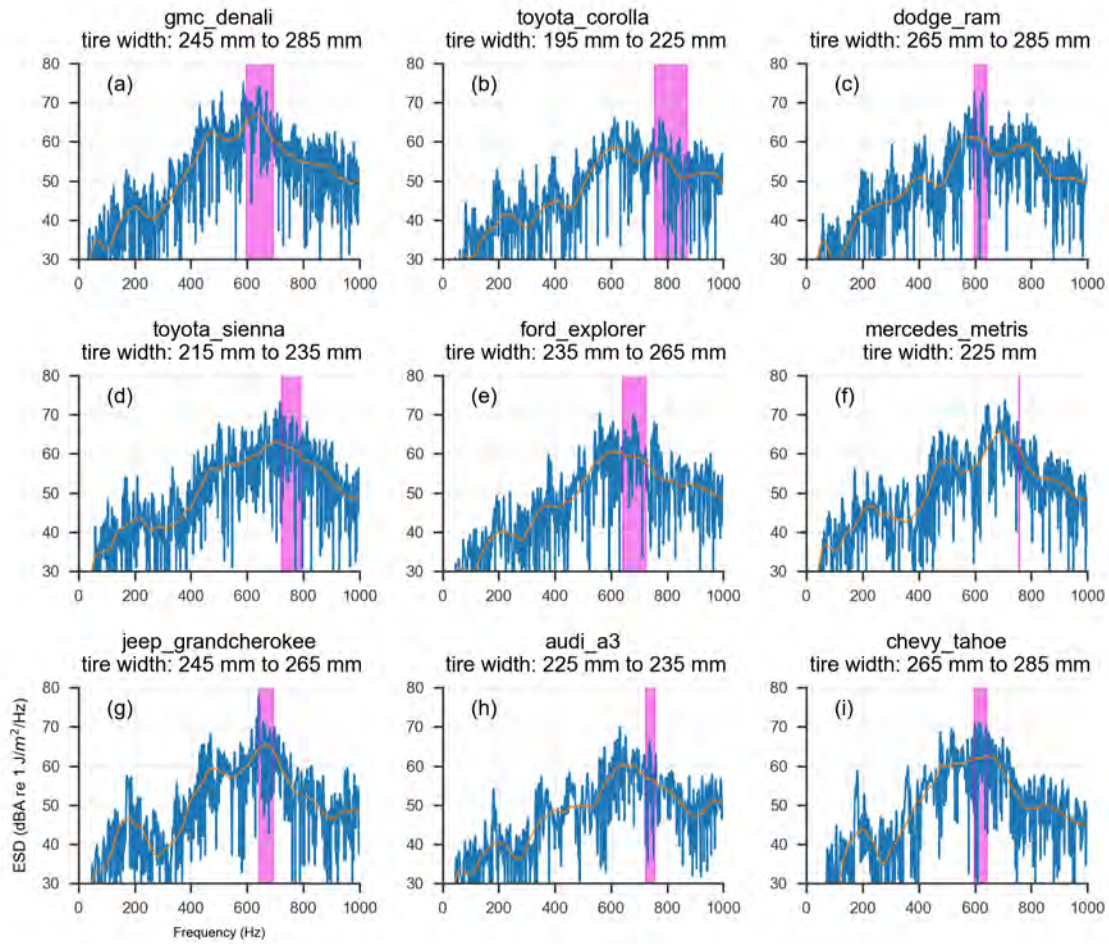


Figure A-5: ESD of car pass events (blue) and ESD with Savitsky-Golay smoothing filter (orange) compared to resonance frequency calculated using Eq. (2)

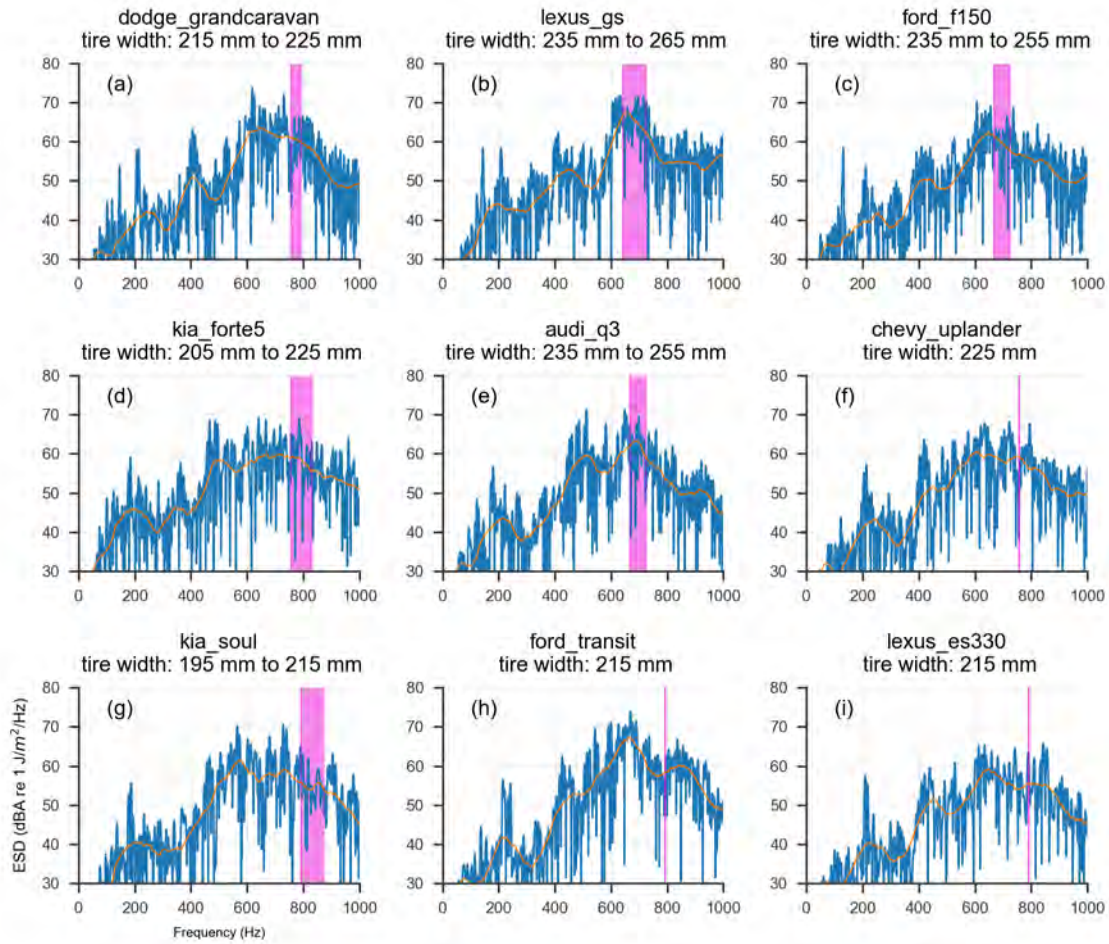


Figure A-6: ESD of car pass events (blue) and ESD with Savitsky-Golay smoothing filter (orange) compared to resonance frequency calculated using Eq. (2)

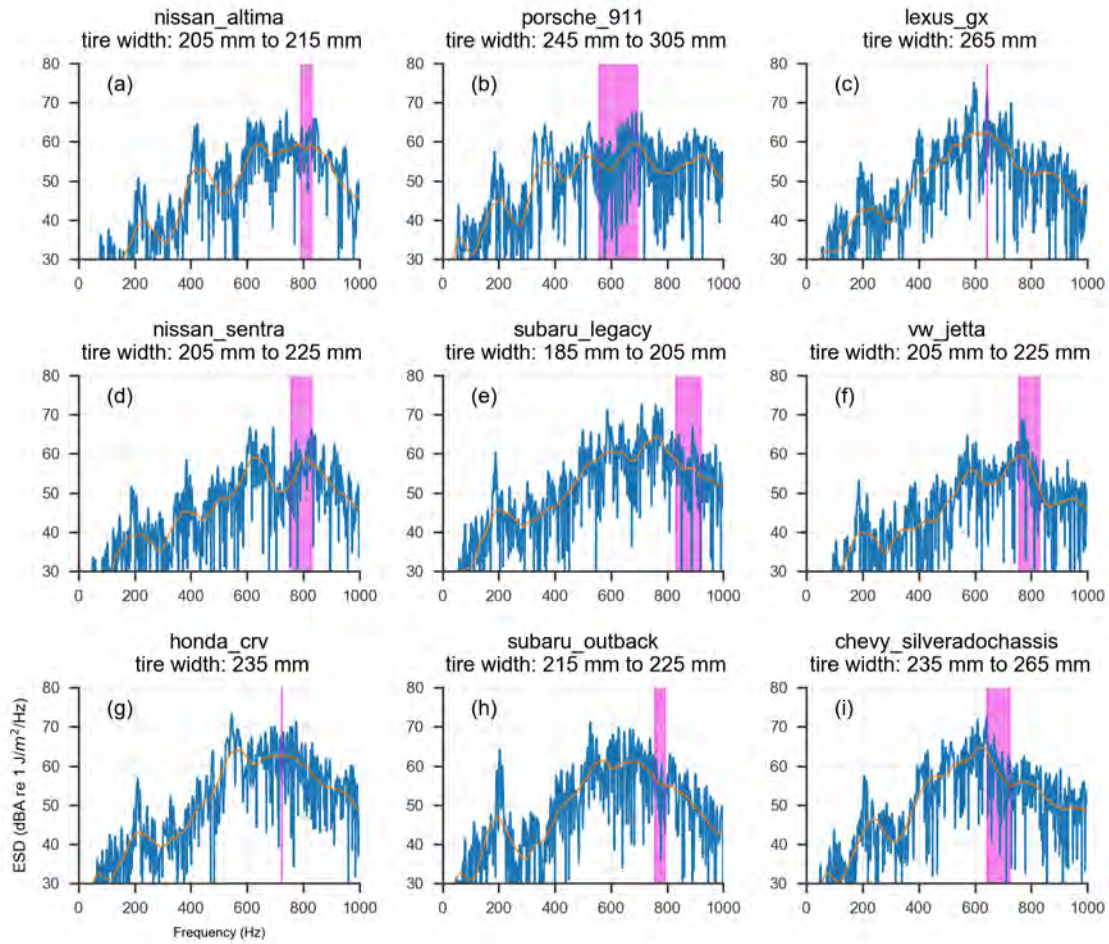


Figure A-7: ESD of car pass events (blue) and ESD with Savitsky-Golay smoothing filter (orange) compared to resonance frequency calculated using Eq. (2)

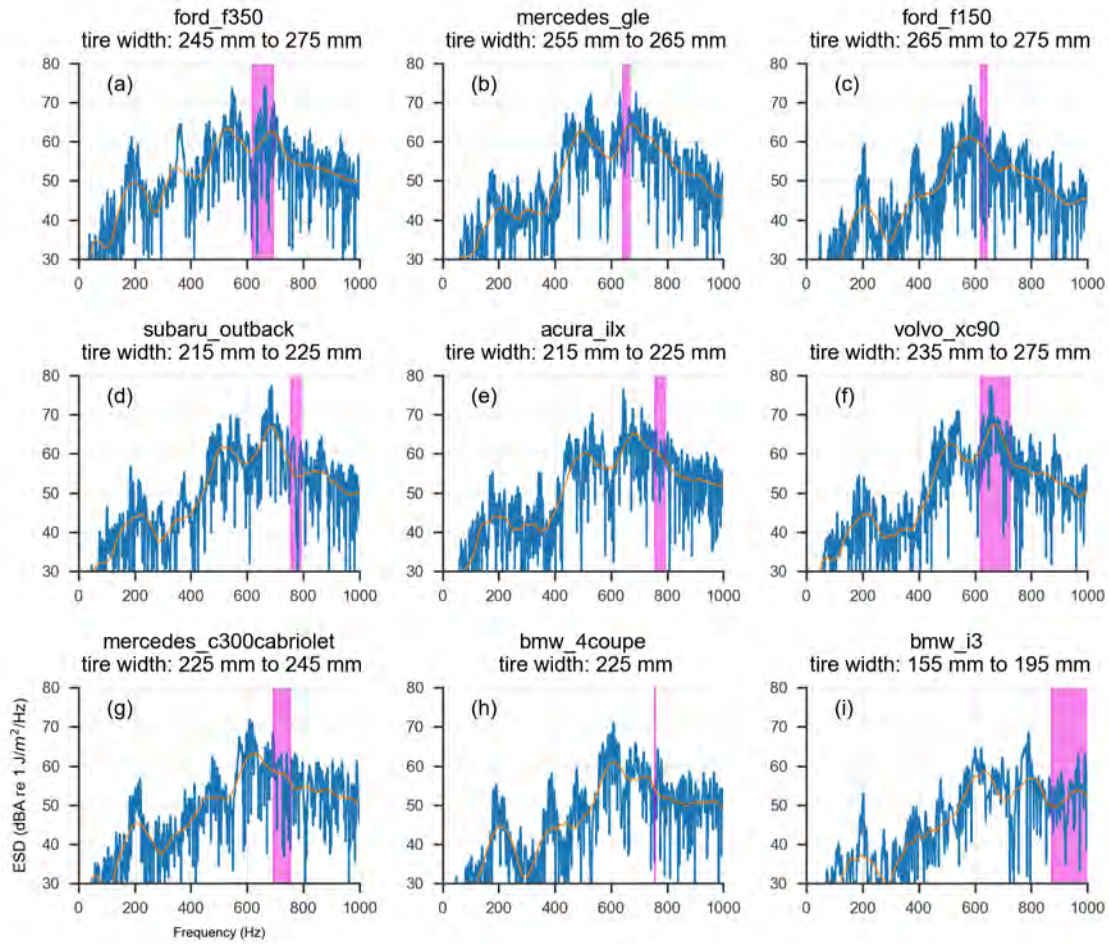


Figure A-8: ESD of car pass events (blue) and ESD with Savitsky-Golay smoothing filter (orange) compared to resonance frequency calculated using Eq. (2)

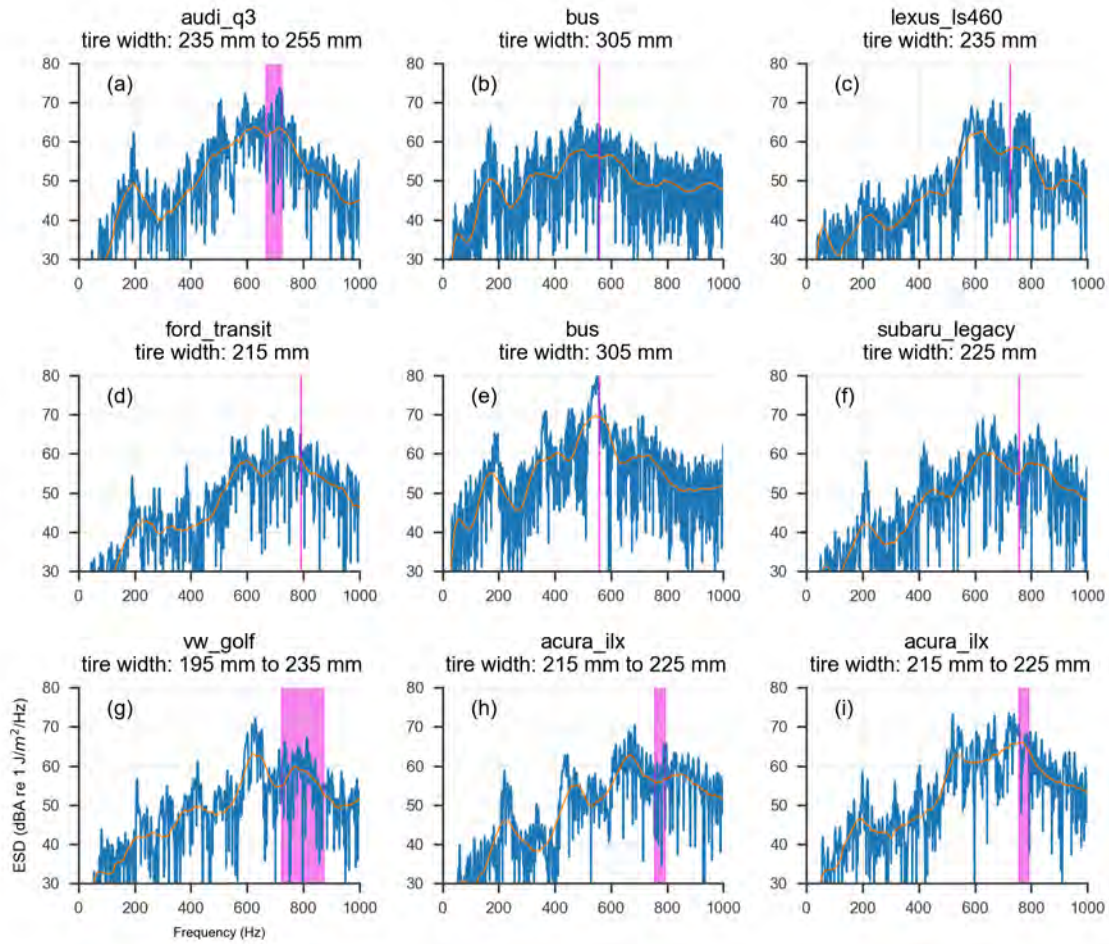


Figure A-9: ESD of car pass events (blue) and ESD with Savitsky-Golay smoothing filter (orange) compared to resonance frequency calculated using Eq. (2)

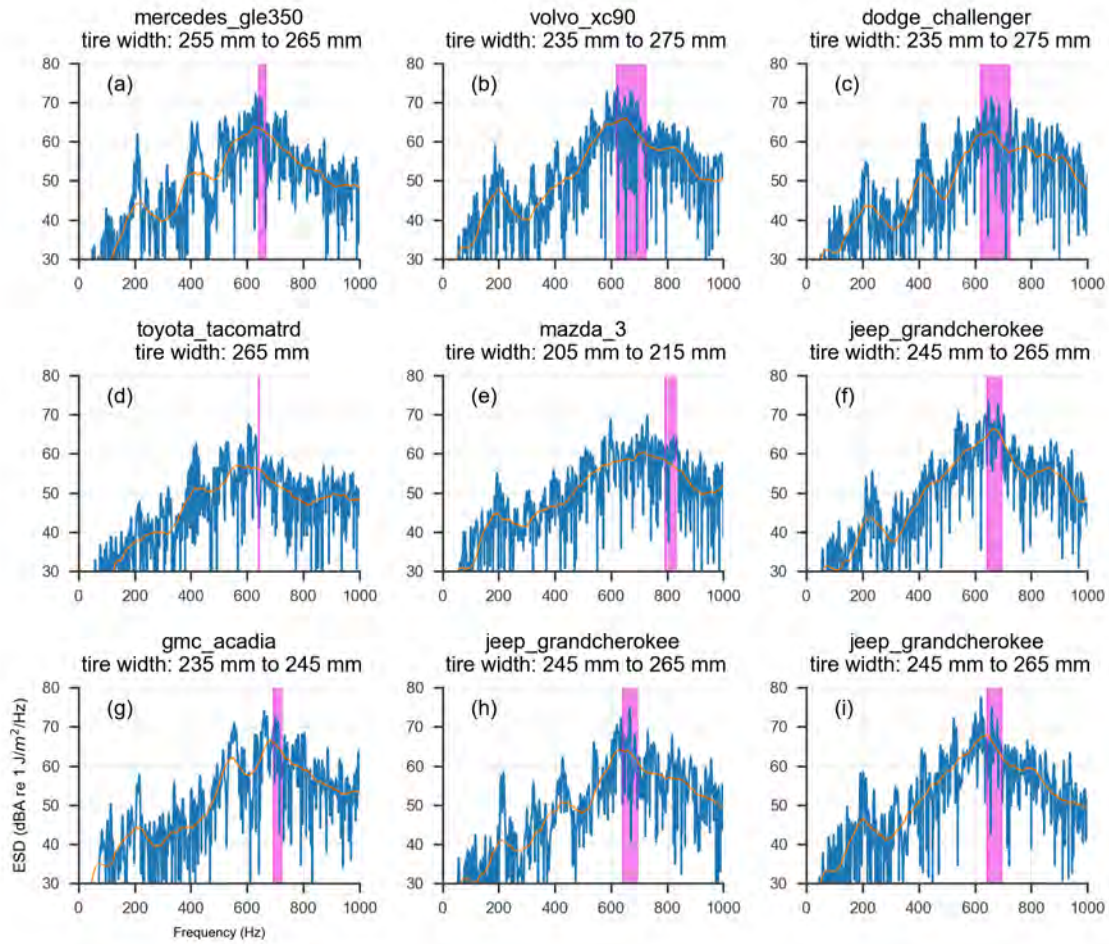


Figure A-10: ESD of car pass events (blue) and ESD with Savitsky-Golay smoothing filter (orange) compared to resonance frequency calculated using Eq. (2)



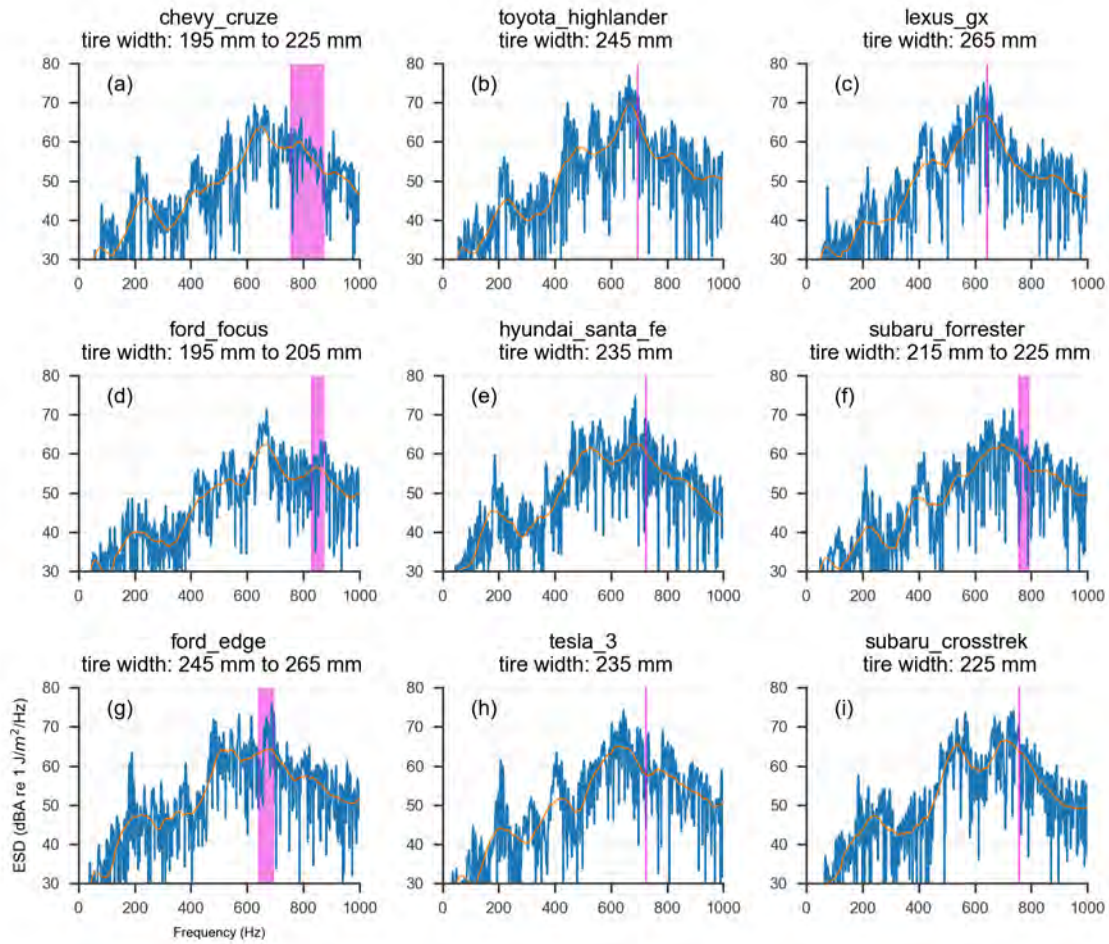



Figure A-11: ESD of car pass events (blue) and ESD with Savitsky-Golay smoothing filter (orange) compared to resonance frequency calculated using Eq. (2)

## Appendix B. Golden Ears Bridge Maintenance Report

PITT MEADOWS		
<b>REPORT</b>	<b>INFORMATION REPORT TO COUNCIL</b>	
<b>DATE:</b> January 11, 2016	<b>FILE:</b> 11-5240-01/16	
<b>FROM:</b> Operations and Development Services Department		
<b>SUBJECT:</b> Golden Ears Bridge – Maintenance Report Request		
<b>RECOMMENDATION: THAT Council:</b>		
A. Receive the report dated February 17, 2016 from the Director of Operations and Development Services for information; OR		
B. Other.		
<b>CHIEF ADMINISTRATIVE OFFICER COMMENT/RECOMMENDATION:</b>		
		
<hr/>		
<b>REPORT/DOCUMENT:</b>	Attached <input checked="" type="checkbox"/>	Available <input type="checkbox"/> N/A <input type="checkbox"/>
<b>PURPOSE:</b> To provide Council the information received from TransLink on February 10, 2016 with respect to the January 19, 2016 Council motion requesting staff to pursue obtaining the maintenance records and maintenance schedule for the Golden Ears Bridge expansion joints from the third party that performed the work.		
<b>BACKGROUND:</b> On May 19, 2015 Council motioned for staff to invite TransLink to attend a Council in Committee meeting to share the test results and standards and maintenance with respect to Golden Ears expansion noise. TransLink responded to this request with a letter included as Attachment A.		
On September 15, 2015 Council motioned that consideration to send a letter under the Mayor's signature to TransLink requesting maintenance reports with respect to noise mitigation inserts be deferred until such times as the response from TransLink is discussed at a future Council in Committee meeting.		
Following receipt of the letter from TransLink, City staff followed up with TransLink staff requesting copies of any maintenance activity records. E-mail communication in October 2015 concluded that TransLink does not have detailed maintenance records.		
<b>NEW COMMUNICATION:</b> On January 30, 2016 staff contacted TransLink requesting the name of the company that performed the maintenance work for the Golden Ears Bridge expansion joints and contact information for someone at the company.		
On February 2, 2016 Susan Chu, TransLink Project Manager, Infrastructure and Network Management, contacted staff to confirm Council's request and offered to make the request on the City's behalf. On February 10, 2016 a letter was received from Ms. Chu with the requested information (Attachment A).		
<b>OTHER CONSIDERATIONS:</b> If Council would like to take any further action.		
- 77 -		
#134558v1		

---

Submitted by: K. Zanon, Director of Operations and Development Services

Approved by: M. Roberts, Acting CAO

**ATTACHMENT(S):**

- A. Letter from Susan Chu, Project Manager, Infrastructure and Network Manager, TransLink, dated February 10, 2016.



**TransLink**

405 - 287 Nelson Street  
New Westminster, BC V3L 0E7  
Canada  
Tel: 779-375-7500

[www.translink.ca](http://www.translink.ca)

South Coast British Columbia  
Transportation Authority

February 10, 2016

Ms. Kate Zanen  
Director of Operations and Development Services  
City of Pitt Meadows  
12007 Harris Road, Pitt Meadows, BC, V3Y 2B5

Dear Ms. Zanen:

**RE: Council motion requesting Golden Ears Bridge maintenance records**

Thank you for your email informing TransLink of the Council motion of January 19, 2016 requesting maintenance records and the maintenance schedule for the Golden Ears Bridge, specifically related to bridge expansion joint maintenance activities.

TransLink has been actively managing the expansion joint noise issue since the Bridge was opened to the public in 2009. It is important to note that the bridge has always met, and continues to meet, all relevant industry standards for noise emissions.

In consultation with local and national independent experts in noise mitigation TransLink actively responded to noise concerns raised by some nearby residents by installing an expansion joint filler solution between 2011 and 2012 to further help with noise mitigation.

This effective solution reduced the noise level by 15% at the bridge joint location, and 18% close to the residences on Wildwood Crescent. This is the equivalent of the noise reduction achieved by inserting industrial earplugs when standing next to the expansion joint.

Additionally, 15-foot high sound deadening fencing was installed on raised berms and speed and noise reduction measures, including larger speed limit signs, use of engine brake signs, additional road markings, and LED speed limit signs were introduced.

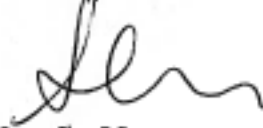
Sound measurements, completed in April 2015, show additional improvements in sound reduction from the previous readings taken in 2012, demonstrating that these changes are working as intended.

The bridge is patrolled every 24 hours and maintenance on the bridge expansion joints takes place on an as-needed basis. TransLink is pleased to provide a log of maintenance activities for the expansion joints (attached).

.../2

TransLink will continue to maintain the expansion joint filler material, and measure the noise emitted to ensure continued performance. We are not considering or planning any other noise mitigation actions.

Yours truly,

A handwritten signature in black ink, appearing to read 'Susan Chu', written over a horizontal line.

Susan Chu, P.Eng  
Project Manager, Infrastructure & Network Management

Attachment: Log of maintenance activities for Golden Ears Bridge expansion joints



**TransLink**  
 400 - 287 Keefer's Court  
 New Westminster, BC V3L 0E7  
 Canada  
 Tel 778.375.1850  
 www.translink.ca  
 South Coast British Columbia  
 Transportation Authority

Log of maintenance activities for Golden Ears Bridge expansion joints

Date	Type of Repair to the Expansion Joints on the Golden Ears Bridge	Quantity of Joints Repaired (m)
February 25, 2013	Temporary repairs* and installation of missing joint material	76.5
February 26, 2013	Temporary repairs and installation of missing joint material	42.2
February 27, 2013	Temporary repairs and installation of missing joint material	6.2
July 13, 2013	Permanent repairs** and installation of missing joint material	31.5
July 12, 2013	Permanent repairs and installation of missing joint material	105
July 11, 2013	Permanent repairs and installation of missing joint material	31.5
July 15, 2013	Permanent repairs and installation of missing joint material	43.8
July 16, 2013	Permanent repairs and installation of missing joint material	30
July 17, 2013	Permanent repairs and installation of missing joint material	49.4
August 23, 2013	Permanent repairs and installation of missing joint material	5

Log of maintenance activities for Golden Ears Bridge expansion joints (continued)

December 23, 2013	Minor repairs	Minor repairs
February 26, 2014	Minor repairs	Minor repairs
March 2, 2014	Minor repairs	Minor repairs
April 11, 2014	Minor repairs	Minor repairs
May 6, 2014	Minor repairs	Minor repairs
July 31, 2014	Permanent repairs and installation of missing joint material	22.5
August 5, 2014	Permanent repairs and installation of missing joint material	23
August 6, 2014	Permanent repairs and installation of missing joint material	39
March 13, 2015	Permanent repairs and installation of missing joint material	45.4
March 16, 2015	Permanent repairs and installation of missing joint material	10.5
March 17, 2015	Permanent repairs and installation of missing joint material	33.7
November 2, 2015	Permanent repairs and installation of missing joint material	18.5
November 3, 2015	Permanent repairs and installation of missing joint material	15
November 9, 2015	Permanent repairs and installation of missing joint material	10.5

\* Temporary repairs are defined as being performed in the winter, when temperatures do not allow for long-term repairs to be made.

\*\* Permanent repairs are defined as performed outside of the winter months to repair the expansion joint for the longer-term.